

Experimental and parametric investigation of castellated steel beam-column in various expansion ratios, lengths and loading conditions

Hanan Hussien El-Tobgy, Anwar Badawy Badawy Abu-Sena, Mohamed Wahied Fares*

Department of Civil Engineering, Faculty of Engineering at Shoubra, Benha University, Cairo, Egypt

ARTICLE INFO

Keywords:

Castellated steel elements
Beam-columns
Expansion ratio
Web opening
FEM modeling
Hexagonal opening

ABSTRACT

This study aimed to investigate the structural behavior of castellated beam-column steel elements. The benefit of castellation laid in increasing the section's depth to induce an increase in the moment of inertia I_x and the section modulus S_x without the slightest increase in the element weight. Most of the previous researches focused on castellated beams but only few concentrated on beam-column elements. An experimental investigation was performed on twelve short and long castellated beams, columns and beam-column elements. The results of the performed experimental work were compared to the finite element analysis (FEA) to validate the applicability of FEA as a numerical tool. FEA was found to be in favorable agreement with their experimental counterparts. In this research, the behavior and strength of the castellated beam, columns, and beam-column elements were investigated by means of the verified finite element modeling. The various parameters taken into consideration in this research were respectively; load eccentricity, element length and castellation ratio.

1. Introduction

Compared to classical I-section elements, castellated elements have superior strength, weight ratio, aesthetic architectural appearance, etc. Therefore, castellated elements are widely used in large span structures such as; stadium, bridges and multi-story buildings. Castellated members are steel I-section members with hexagonal openings located at fixed distances along the web. They are usually prepared by cutting a hot-rolled I-section member according to a polygonal pattern, afterwards, both halves are shifted and once again welded together as shown in Fig. 1. The resulting castellated member is typically 40–60% deeper than its original parent section, hence, remarkably increasing the strong-axis bending resistance. By varying the cutting pattern and the properties of the parent sections, a wide variation of opening shapes and beam geometries becomes possible, such as cellular or tapered members.

Mohebkhah and Showkati [1] studied the effect of lateral bracing on castellated steel element capacities and concluded that the effect of bracing became reduced in the elastic buckling range, whereas this effect is enhanced with the increase of the laterally unbraced length. They developed a general equation to predict the castellated flexural members' stiffness and capacity. The developed formula accounted for the member slenderness. Showkati [2] investigated the behavior of castellated steel beams without the provision of lateral supports. He

developed empirical equations that could be used to estimate the coefficient of bending (C_b) for castellated-beams under various conditions.

Ellobody [3,4] studied the effect of combined lateral-torsional and distortional buckling modes on the behavior of castellated and cellular elements. In his study, he considered normal and high strength steel castellated elements and concluded that failure load of castellated steel elements was likely reduced due to the presence of web distortional buckling in the case of slender steel beams. He also, found out that, utilizing high strength steel has contributed to an increase in the failure load of less slender castellated beams. He furthermore concluded that the Australian Standards equations predicting the behavior of steel beams under lateral-torsional buckling were conservative, however, when castellated elements were failing in web distortional buckling the equation was otherwise. Finally, when high strength beams by lateral-torsional buckling, the AS expressions were quite conservative.

Abu-Sena et al. [5] conducted a parametric study to predict the buckling behavior and the element capacity of beam-column elements. They considered the initial imperfection in the F.E.A and developed an analytical model to predict the interactive strength compared to the finite element non-linear analysis of EC3 design approach. Yuan et al. [6] studied the critical buckling load of simply supported castellated columns. They considered the buckling about the major axis and

* Corresponding author.

E-mail address: engwahed2008@gmail.com (M.W. Fares).

<https://doi.org/10.1016/j.istruc.2021.04.053>

Received 24 December 2020; Received in revised form 21 February 2021; Accepted 18 April 2021

Available online 5 May 2021

2352-0124/© 2021 Institution of Structural Engineers. Published by Elsevier Ltd. All rights reserved.

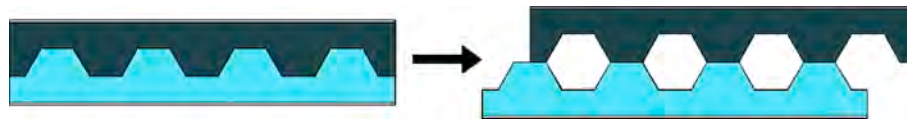


Fig. 1. Standard fabrication method of castellated members starting from a plain-webbed parent section.

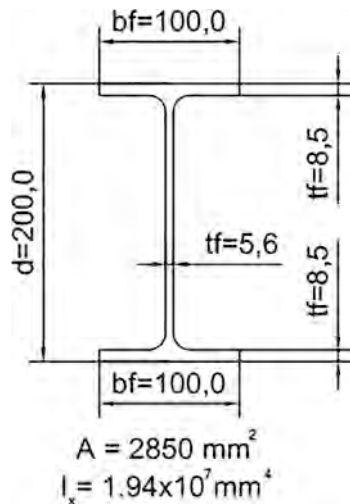


Fig. 2. IPE200 Cross-section used for experimental work in this research.

concluded that the presence of the web openings resulted in shear deformations along the castellated steel column and contributed to reduction in the buckling capacity of the castellated steel column. They moreover concluded that web shear deformations couldn't be neglected, even if the second moment at the opening location's area was taken into consideration in predicting the buckling strength of the castellated steel column.

Kumbhar and Jamdar [7] investigated the behavior of castellated elements with sinusoidal openings. They used these types of openings to study the possibility of optimization. They considered different sizes of web openings and found that when sinusoidal web opening sizes were

Table 1
Test Matrix of Castellated Specimens Tested in Groups I, II and III.

Group	Specimen ID	L_{act} (mm)	L_{eff} (mm)	$\lambda_y = \frac{L}{r_y}$	Castellation Ratio (R)	e/d
I	L17-R1.3-e0.0	1732.1	1462.1	66	1.3	0.0
	L17-R1.5-e0.0	1847.5	1577.5	71	1.5	0.0
	L30-R1.3-e0.0	2979.1	2709.1	121	1.3	0.0
	L30-R1.5-e0.0	3233.2	2963.2	133	1.5	0.0
	L17-R1.3-e0.50	1732.1	1462.1	66	1.3	0.5
II	L17-R1.5-e0.50	1847.5	1577.5	71	1.5	0.5
	L30-R1.3-e0.50	2979.1	2709.1	121	1.3	0.5
	L30-R1.5-e0.50	3233.2	2963.2	133	1.5	0.5
	L17-R1.3-e0.75	1732.1	1462.1	66	1.3	0.75
	L17-R1.5-e0.75	1847.5	1577.5	71	1.5	0.75
III	L30-R1.3-e0.75	2979.1	2709.1	121	1.3	0.75
	L30-R1.5-e0.75	3233.2	2963.2	133	1.5	0.75

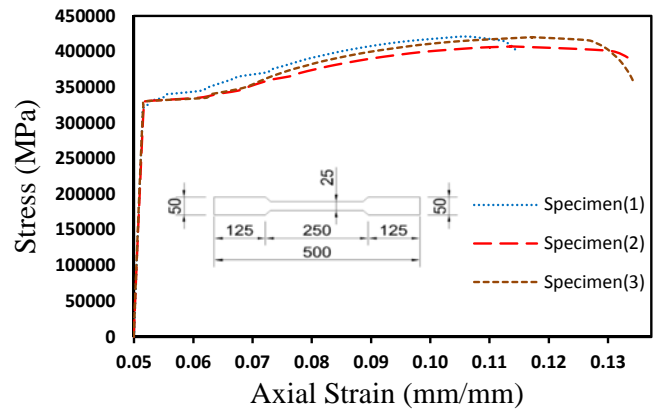


Fig. 3. Tensile Stress-Strain Curve of Specimens.

equal to 0.55 times the total depth of the beam element, along with the strength of the element might reach the maximum. They also concluded that utilizing these types of openings resulted in further shear transfer area. Gu and Cheng [8] studied the critical buckling load (CBL) of cellular columns. They focused on the major buckling axis and considered the web shear deformations that have a clear influence on the buckling capacity of the cellular elements. They concluded that the effect of shear deformations on the cellular element increased along with the increase in the cross-section area of the tee section above the openings and the diameter of the web opening, however it decreased with the web thickness and the length of the cellular element.

Shaikh and Autade [9] studied the effect of web shear deformation on the critical buckling load of castellated beams. They found out that, the depth of the web openings had a significant effect on the shear deformations that might occur in the castellated steel element. They also presented an analytical solution to predict the critical buckling load of the castellated steel element and found out that the utilization of rounded holes avoided Vierendeel effect (to avoid stress concentration), and local failure of the beam. The provision of a plate below the concentrated load and reinforcement at the beam's weak sections could be used to enhance the beam's capacity. Sonck and Belis [10] studied the effect of residual stresses on the weak-axis flexural capacity of both castellated and cellular columns. They concluded that the weak axis flexural capacity was affected by the residual stress simulation.

Wang et al. [11] used the finite element method to investigate the post-buckling behavior of the web of castellated beams when subjected to vertical shear. They concluded that the web thickness and the inclination angle of the web opening had a significant effect on the shear

Table 2
Material Properties as per the coupon test results.

Coupon	Width (mm)	Thick (mm)	Initial Length (mm)	Elastic Modulus E(GPa)	Yield Strength (MPa)	Ultimate Strength (MPa)
Specimen (1)	21.7	6.1	221.6	186.4	331	421
Specimen (2)	23.9	6.1	221.4	189.6	321	407
Specimen (3)	23.8	5.85	211.2	213.8	303	420
Average	23.13	6.017	218	197	319	416

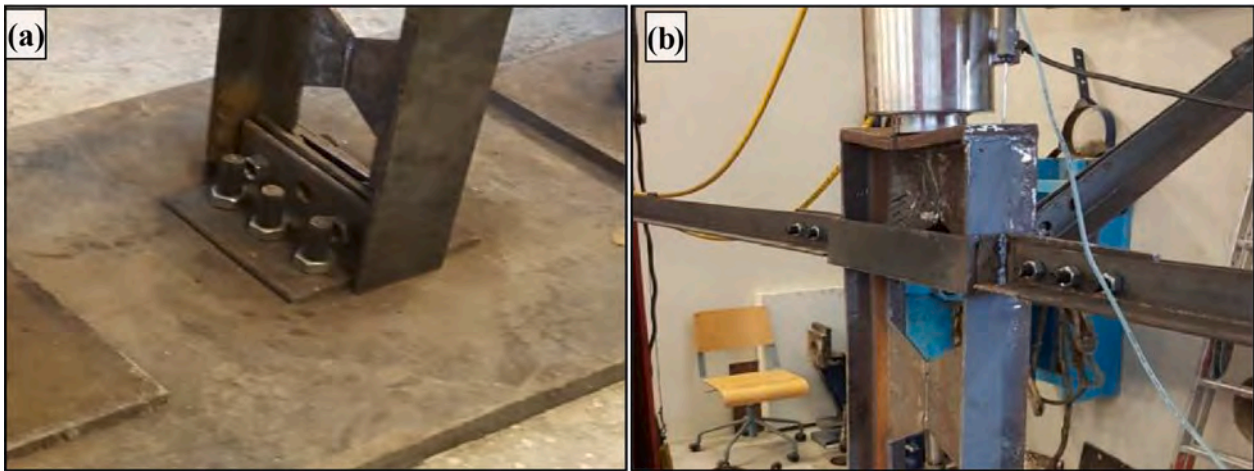


Fig. 4. Specimen ends connection: (a) Lower end connection; (b) Upper end connection.

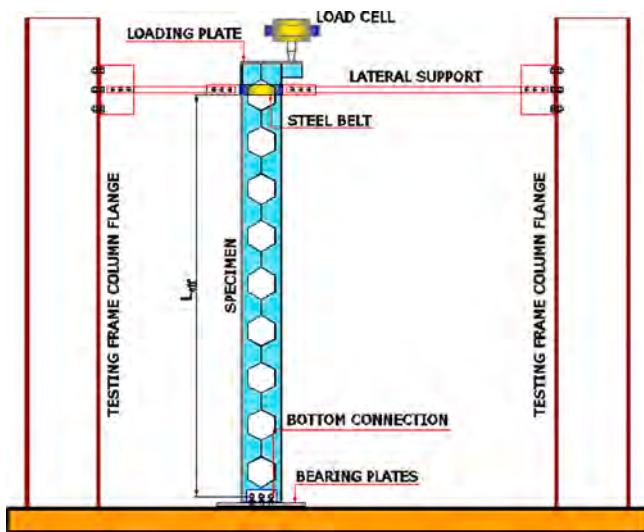


Fig. 5. Test setup.

buckling factor. They moreover presented a simplified method to predict the shear buckling factor of castellated steel beam. Yuan et al. [12] investigated the transverse deflection of perforated beams. They considered two different boundary conditions and concluded that web

shear effect could significantly increase the transverse deflection of castellated and cellular beams particularly when the beam has a short length and deep section.

Elaiwi et al. [13] presented theoretical and numerical solutions for calculating the deflection of hexagonal castellated beams with simply supported boundary condition, considering the influence of shear deformations that might occur in the web. Elaiwi et al. [14] investigated the effect of the web opening on the lateral-torsional buckling resistance of castellated beams. They developed an analytical solution that could be used for the design and practicality. They concluded that plastic failure was the failure of short castellated beams' mode whereas lateral-torsional buckling was the mode of long beams' failure, accordingly, the longer the beam, the less important was the nonlinearity.

Hadeed and Alshimmeri [15] studied the effect of castellated with and without strengthening on the structural behavior of castellated-beams and compared the results with the origin solid steel beam. They found out that, the load carrying capacity of the castellated steel beams was increased compared with the original solid beam, while mid-span deflection values at service load were decreased comparing with the origin solid steel beam. Serene and Aswathy [16] presented finite element analysis of composite beams and columns with castellated members of full height web openings. They considered different shapes of web openings namely rectangular, hexagonal and elliptical in partially and fully encased with concrete. They concluded that elliptical web opening was efficient for the improved behavior.

Liu et al. [17] studied octagonal web openings elements. They used

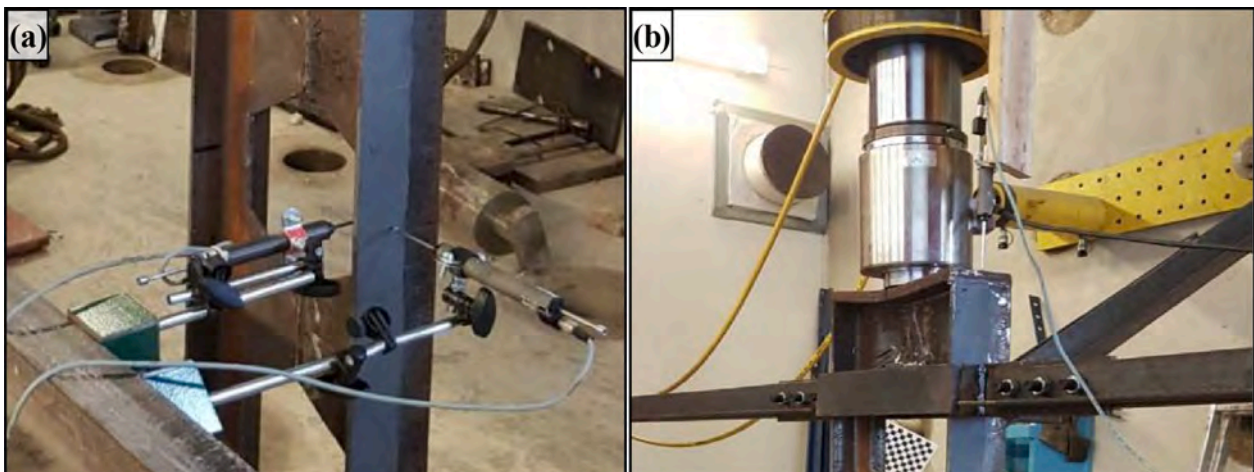


Fig. 6. Arrangement of LVDTs of Group I: (a) Horizontal LVDTs of Group I; (b) Vertical LVDT of Group I.



Fig. 7. Arrangement of LVDTs of Groups II&III: (a) Horizontal LVDTs of Groups II&III; (b) Vertical LVDT of Groups II&III.

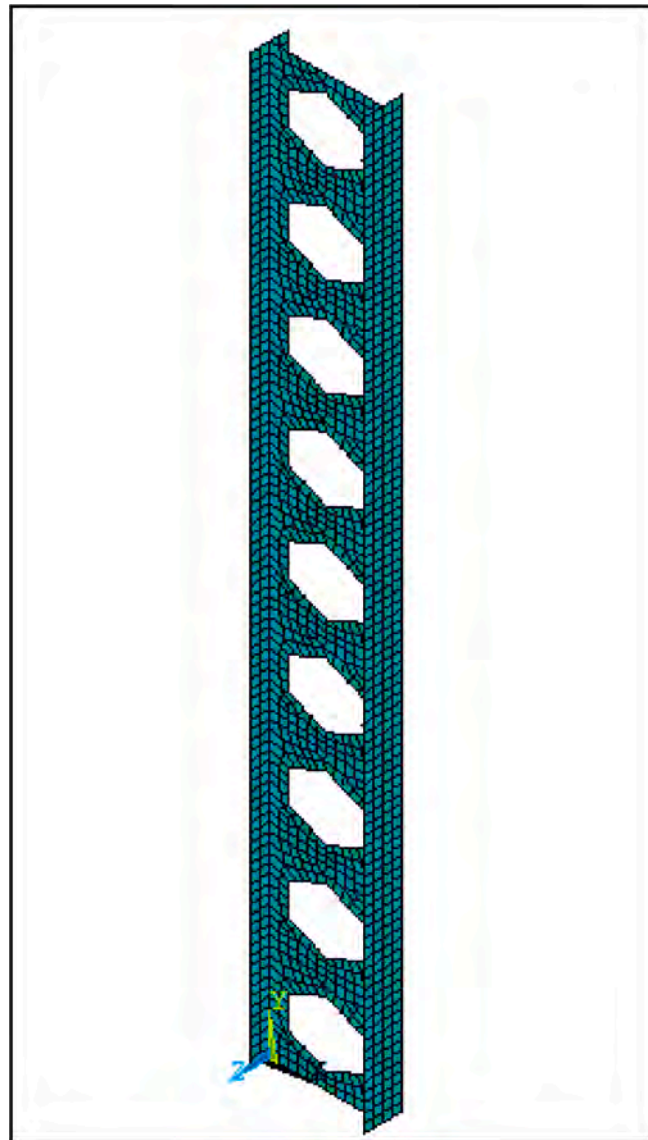


Fig. 8. Steel column modeled as SHELL91.

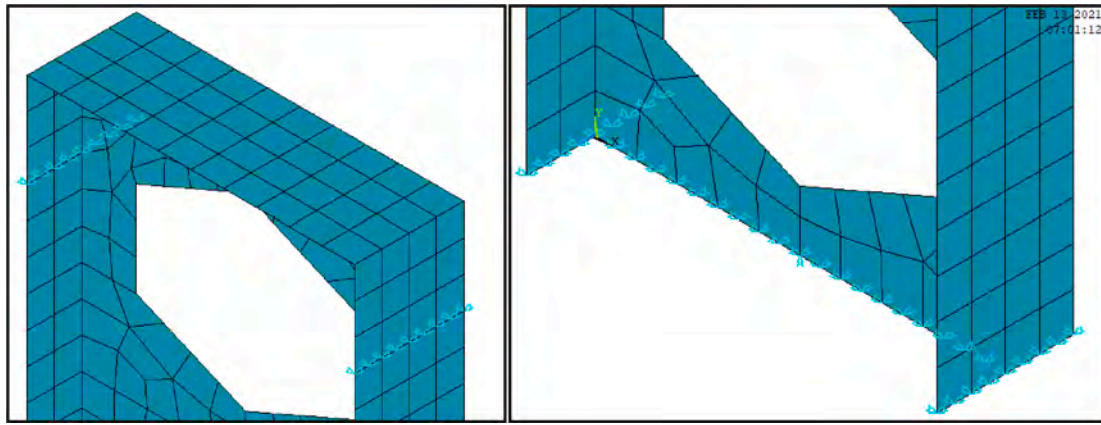


Fig. 9. Top and bottom boundary conditions.

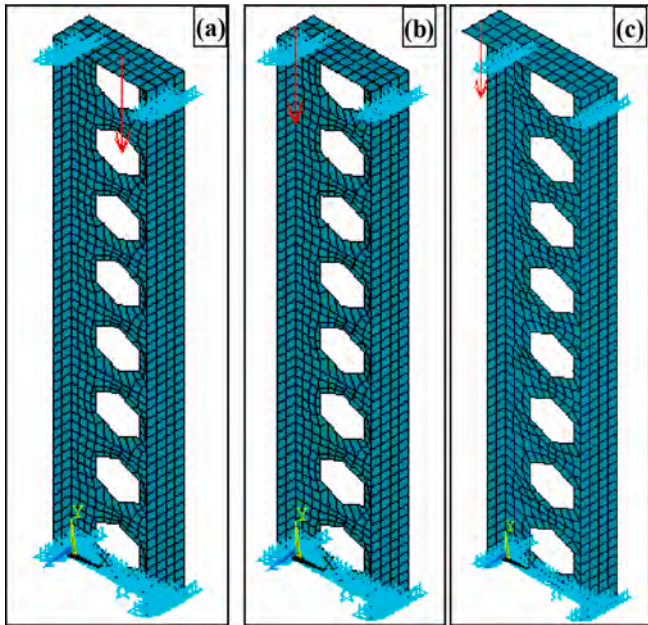


Fig. 10. Created models for L17-R1.3 elements: (a) L17-R1.3-e0.0; (b) L17-R1.3-e0.50; (c) L17-R1.3-e0.75.

high strength bolt to connect the two halves of the elements in site instead of utilizing the factory welding. They draw a comparison between bolted and welded web opening elements and found out that, the structural behavior of bolted elements was further improved than the welded elements.

Considerable amount of research has investigated the behavior of castellated steel beams and/or columns. However, most of these studies were confined on the lateral-torsional buckling of castellated steel beams, types of openings (either circular or hexagonal web openings), the buckling behavior of castellated steel columns and the deflection of castellated beams. Nevertheless, no research seemed to have investigated the behavior of castellated steel beam-column elements. Therefore, this study will have the precedence in contributing towards the implementation of castellated beam-column elements into numerous structures such as office buildings, car parks, shopping centers, hospitals almost any structure with a suspended floor.

This paper reports on short and long castellated steel beam, column and beam-column elements. Experimental study was developed to examine the behavior of castellated steel beam-column elements. Linear interaction diagrams were plotted to illustrate the effect of castellation on linear buckling behavior of castellated elements. Also, non-linear interaction diagrams were plotted to investigate the effect of castellation on the element capacity. This paper presents different castellation ratios (R), where R equals the ratio between castellated element and the original solid web element. Therefore, enhancement diagrams were plotted to investigate the best castellation ratio, enhancement diagrams plotted.

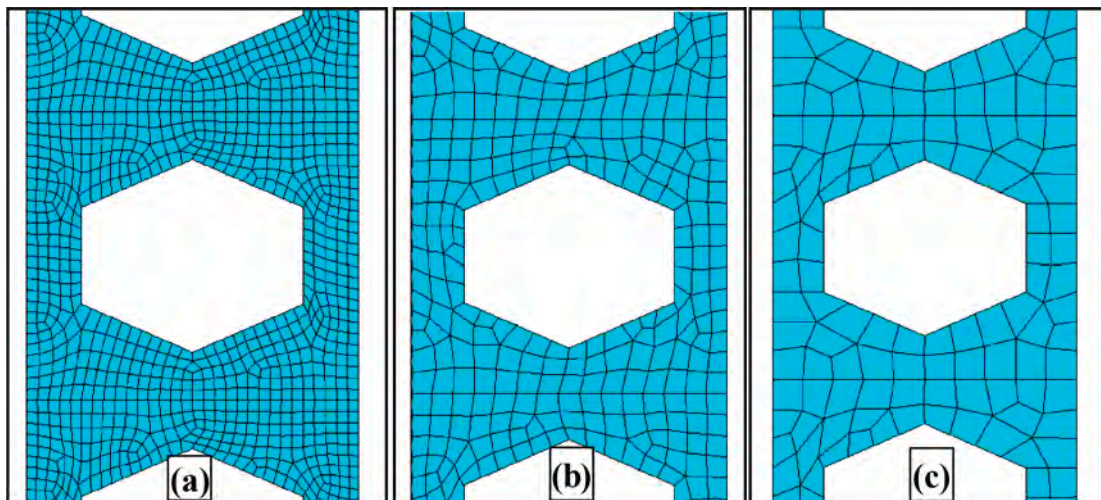


Fig. 11. Mesh convergence used for verified model: (a) 10 mm mesh size; (b) 20 mm mesh size; (c) 30 mm mesh size.

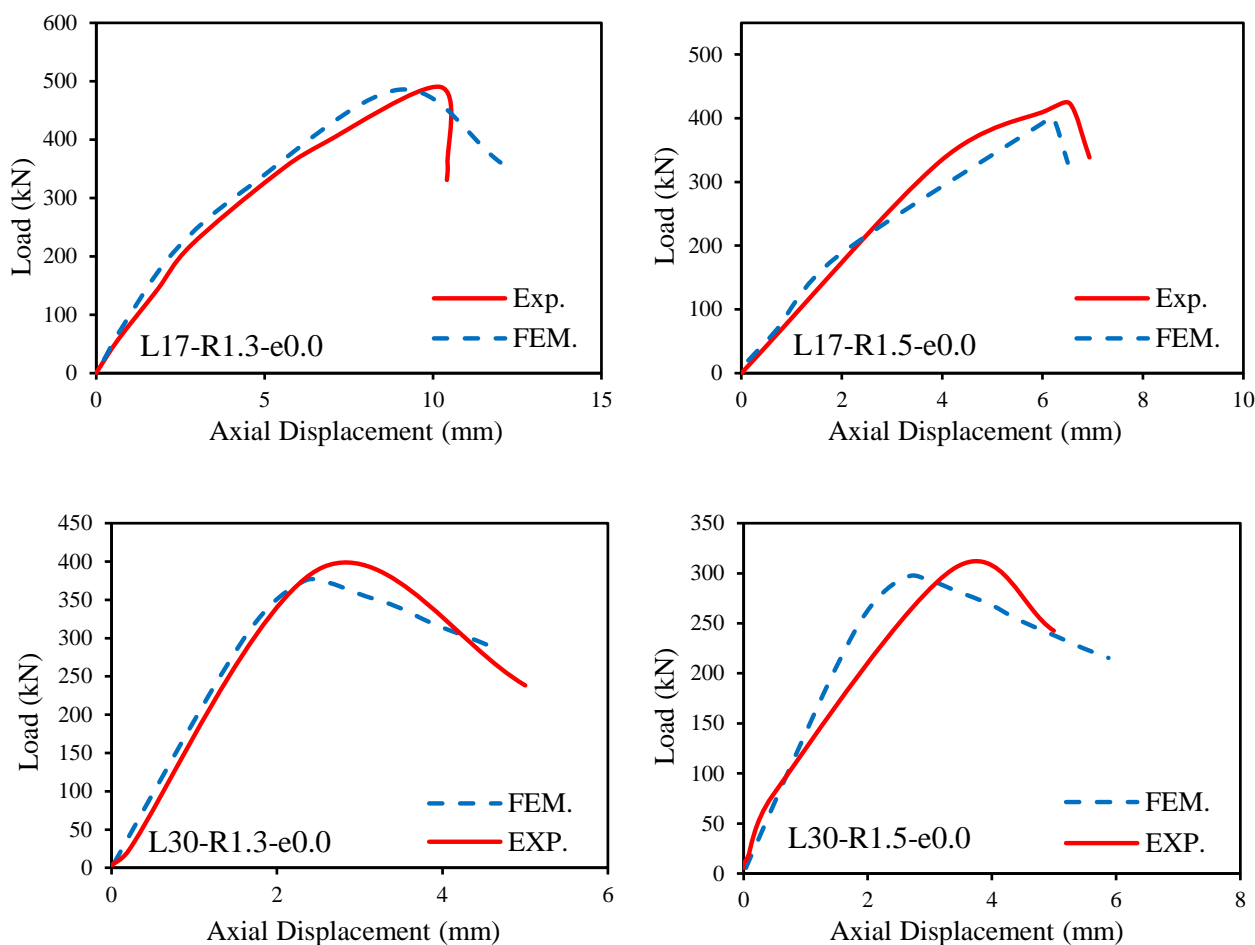


Fig. 12. Load-axial displacement curves of pure axial columns.

The main purpose of the current study was to investigate the effect of castellation on the beam-column elements, examining short to long castellated elements with six different eccentricity ratios, (e/d), where “e” represented the load eccentricity and “d” the section depth. The studied (e/d) ratios are; 0, 0.25, 0.5, 0.75, 2.0 and infinity. The (e/d) = 0, represents the pure axial elements to study castellated column where, (e/d) ratios from 0.25 to 2.0 represents eccentric elements to study beam-column elements and (e/d) = ∞ represents pure bending elements to study castellated beams. Four castellation ratios (R) were considered in the study; 1.0 (solid web elements), 1.3, 1.4 and 1.5. Castellation Ratio (R = 1) was chosen to study the effect of castellation in comparison with the solid web elements, where other castellation ratios were chosen to investigate the best one to improve the element behavior and strength. Four element lengths for both original and castellated elements were taken into consideration; 1.7 m represented the short elements, 2.2 & 3.0 m the intermediate elements, and 4.0 m the long elements. One of the commercially available IPE sections was chosen carefully with the standard section dimensions as shown in Fig. 2 and utilized in the experimental work and the parametric study.

The study consisted of two stages; first stage based on the eigen value buckling analysis and development of the interaction linear buckling diagrams to investigate the effect of castellation on the critical buckling load. The second stage considered the non-linear buckling analysis and development of the interaction diagrams to monitor the effect of castellation on the element capacity.

The castellated element was titled according to its length followed by castellation ratio (R) subsequently the (e/d) ratio, for example L30-R1.5-e0.75, a castellated element that has a length of 3000 mm, castellation ratio (R) = 1.5 and (e/d) = 0.75.

2. Experimental study

2.1. Experimental program

Twelve specimens were tested to study the effect of castellation on the beam-column elements behavior and strength.

The experimental program consisted of 3 groups. Group I, focused on the axial compression behavior of 4 short and slender I-section columns. The parameters taken into consideration were; the effect of castellation ratio (R) and the slenderness ratio of the steel columns. The columns were instrumented to examine their behavior in terms of the load-axial displacement and load-lateral displacement responses.

Groups II-III, were focused on the axial-flexural behavior of 8 short and slender I-section beam-columns. The parameters considered were the effect of castellation ratio (R), the slenderness ratio of the steel sections and the eccentricity to section depth ratio (e/d ratio). Group II was focused on the structural behavior of 4 short and long I-beam-column sections in ratio of $e/d = 0.5$, while group III was focused on the structural behavior of 4 short and long I-section members in ratio of $e/d = 0.75$. The I-sections were instrumented to examine their behavior in terms of the load-axial displacement and load-lateral displacement response. Effective length of each specimen is measured from the bottom of the upper lateral restraint to the bolts of the lower restraint as shown in Fig. 5. The parameters of each group are shown in table 1.

2.2. Coupon test

Three tensile coupon tests were performed to specify the mechanical characteristics of tested steel specimens. The representative stress-strain

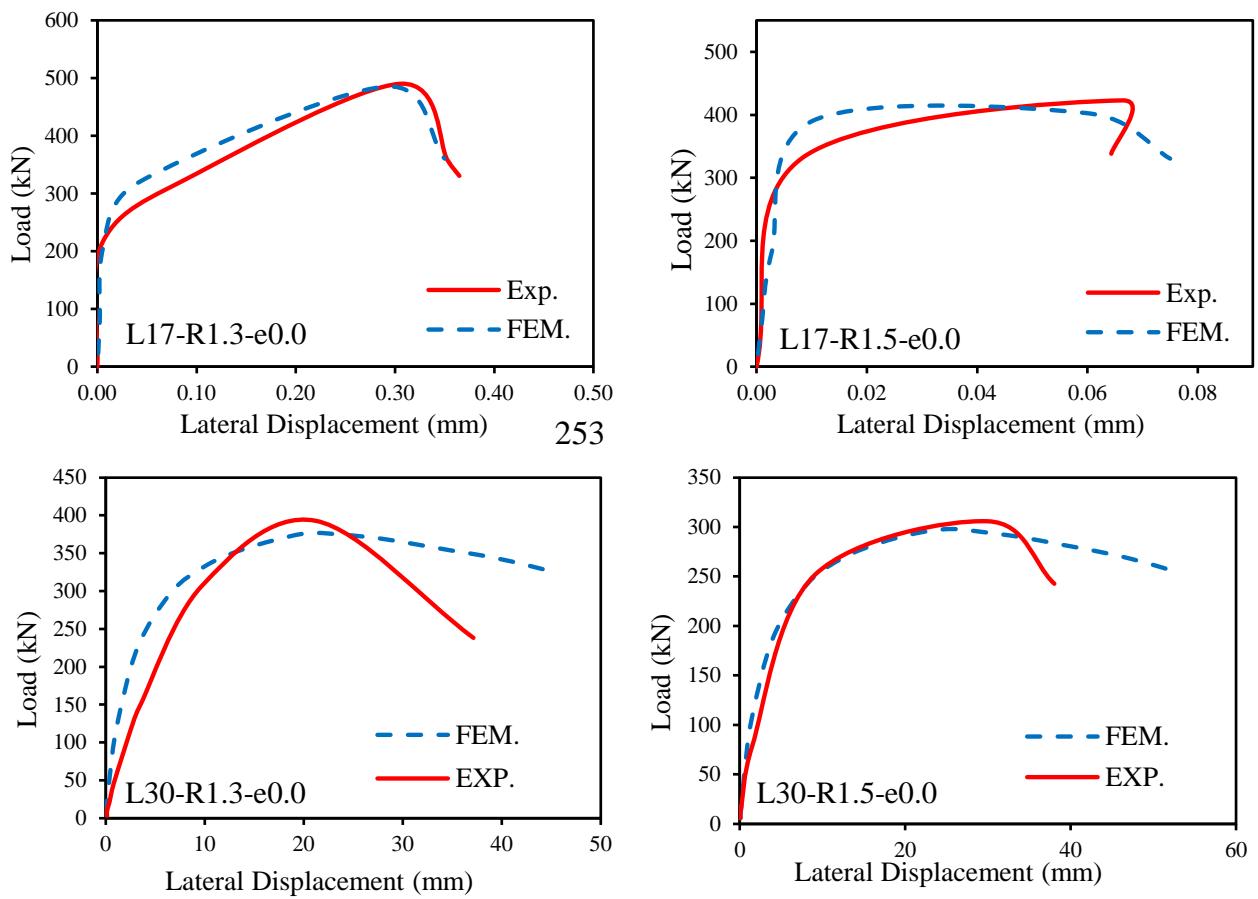


Fig. 13. Load-lateral displacement curves of pure axial columns.

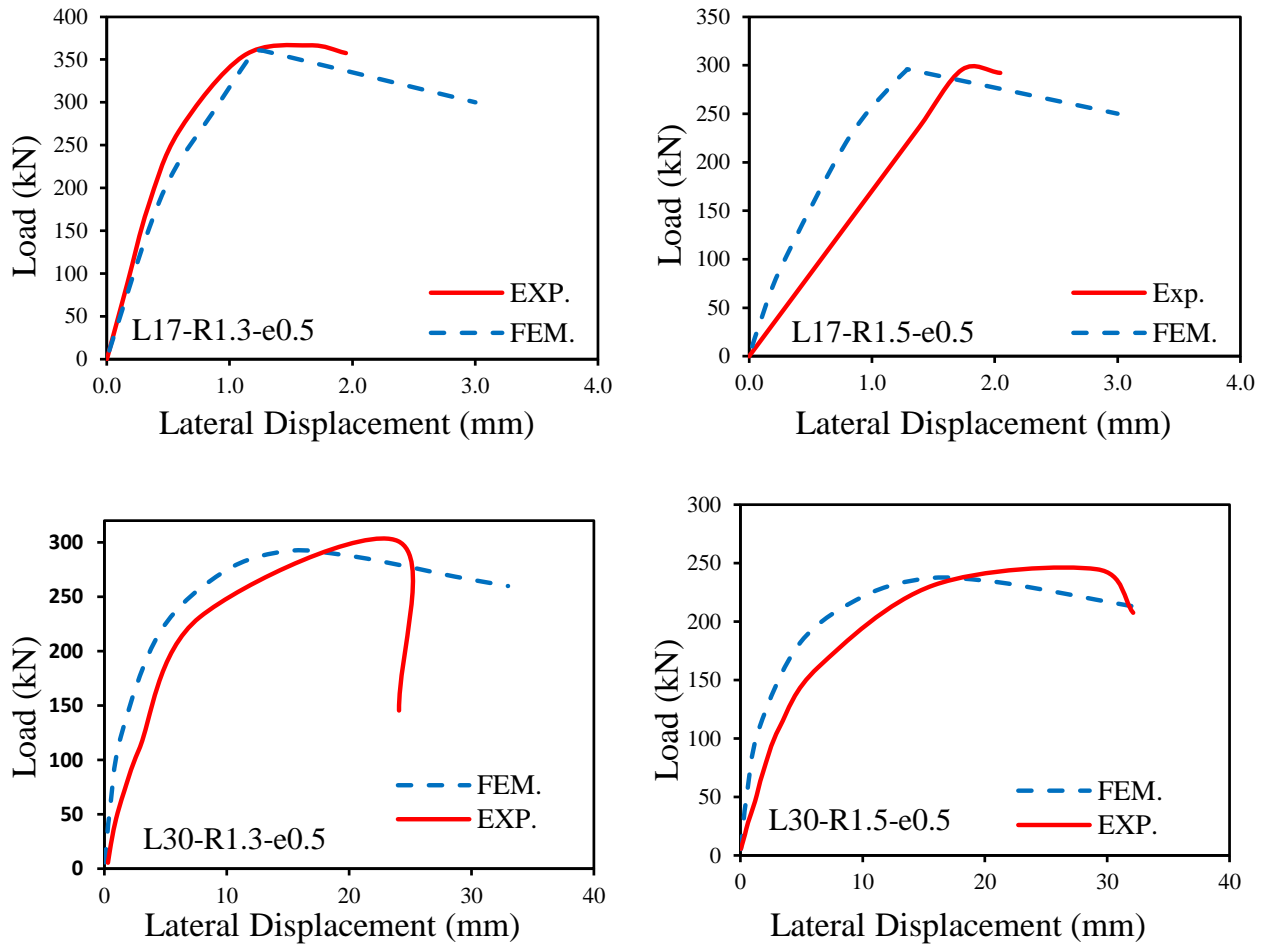


Fig. 14. Load-displacement curves of beam-column elements ($e/d = 0.5$).

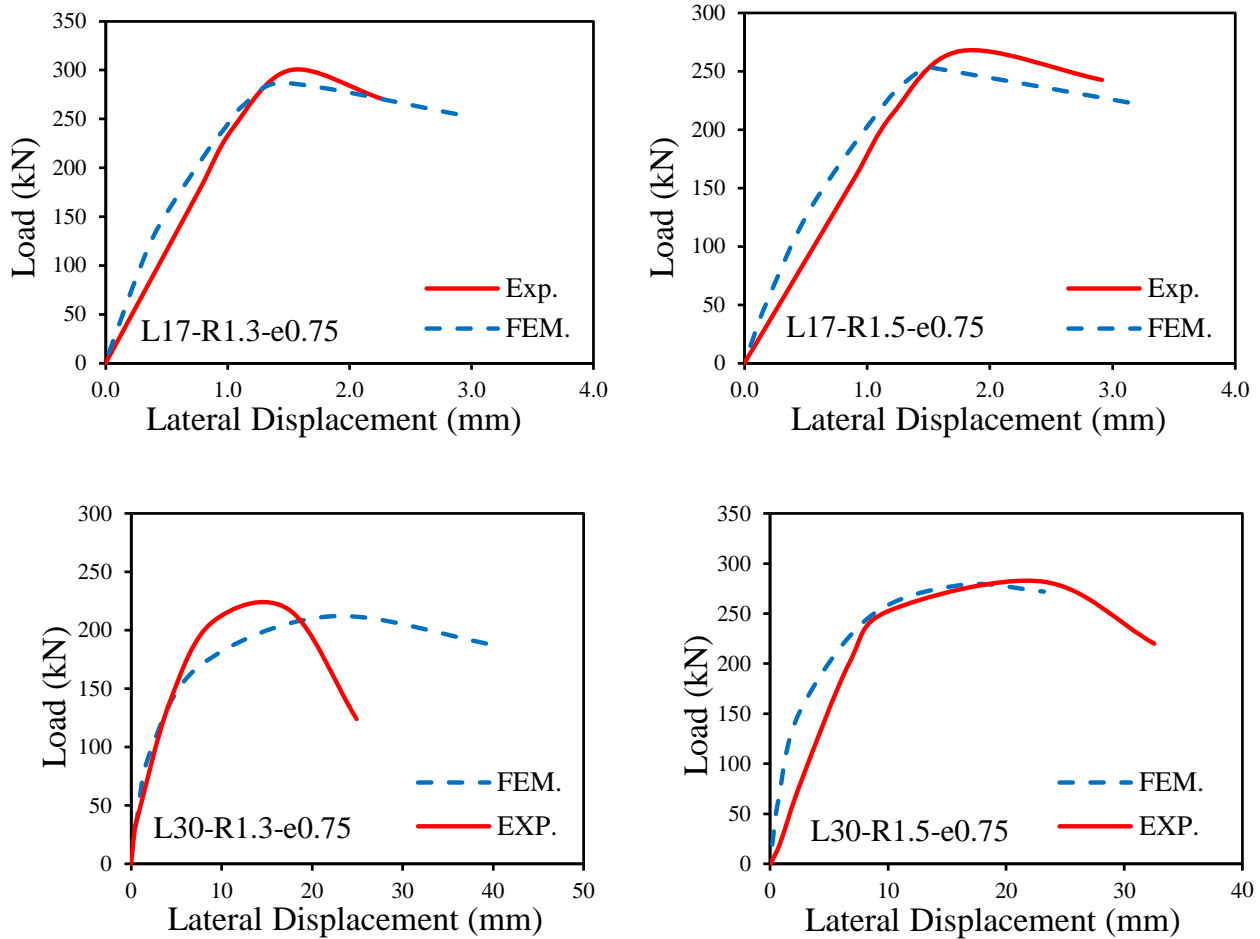


Fig. 15. Load-displacement curves of beam-column elements ($e/d = 0.75$).

Table 3
Comparison between Experimental and Finite Element Ultimate Capacities.

Group	Specimen ID	Ultimate compressive Load (kN.)		Exp./F.E.
		Exp.	F.E.	
I	L17-R1.3-e0.0	490.11	485.12	1.01
	L17-R1.5-e0.0	423.17	402.71	1.05
	L30-R1.3-e0.0	392.7	376.68	1.04
II	L30-R1.5-e0.0	305.81	297.82	1.03
	L17-R1.3-e0.50	366.74	360.27	1.02
	L17-R1.5-e0.50	295.65	295.84	1.0
III	L30-R1.3-e0.50	301.3	292.06	1.03
	L30-R1.5-e0.50	244.87	236.94	1.03
	L17-R1.3-e0.75	300.17	286.88	1.05
III	L17-R1.5-e0.75	267.44	253.19	1.06
	L30-R1.3-e0.75	282.11	278.5	1.01
	L30-R1.5-e0.75	217.8	211.88	1.03
Mean (μ)				1.03
Standard deviation (S)				0.017
Coefficient of variation (V) = S/μ				0.0165

curves of all tested specimens are shown in Fig. 3. Mechanical properties of the tested steel specimens are shown in Table 2.

2.3. Test setup

The end boundary conditions were pinned-pinned, so the specimen from one end was supported on the bearing plates by a simple connection to permit rotation, while, the upper end of the specimen was supported by using steel elements that also permitted rotation. The top

lateral restraint was at a distance of 50 mm down away from the load applying position, therefore the specimen was permitted to move down without any resistance from the lateral supports. Also, out of plan movement was restrained by using lateral support to ensure specimen out of plan stability. Fig. 4 illustrates the end boundary conditions used in the experimental work.

All specimens were tested under vertical load using one test setup as shown in Fig. 5. Testing machine capacity was 1000 kN. Load cell position was based on e/d ratio. The column elements load cell was on the top center of the specimen while elements of the load cell for beam-column were eccentric to satisfy the required e/d ratio.

For group I, three LVDTs were used; one of them was mounted at the top loading plate to measure the vertical displacement, where the other two LVDTs were mounted at the mid-height to measure the lateral displacements as shown in Fig. 6. For groups II and III four LVDTs were used; one of them was mounted at the top loading plate to measure the vertical displacement, where three LVDTs were mounted at the mid-height to measure the lateral displacements and the rotations as shown in Fig. 7.

3. Finite element simulation

3.1. Finite element model

Behavior and strength of castellated beam-column is investigated utilizing the finite element analysis applying ANSYS software [18]. The current study considered linear and non-linear buckling analysis. SHELL91 element was used to model both flanges and web as appropriate for modeling thin to moderately thick shell structures. It was 8-

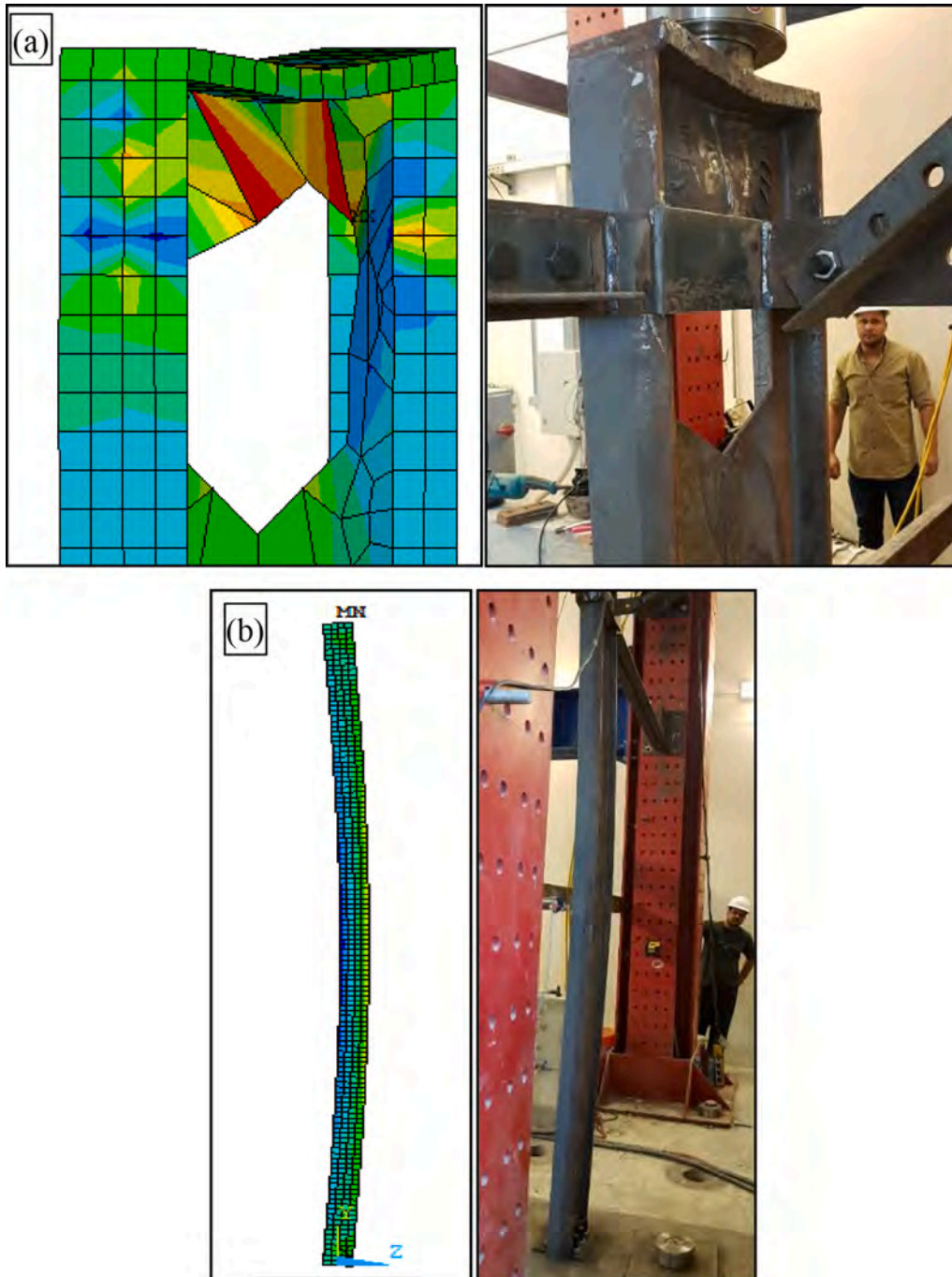


Fig. 16. Modes of failure of pure axial columns: a) short columns; b) long columns.

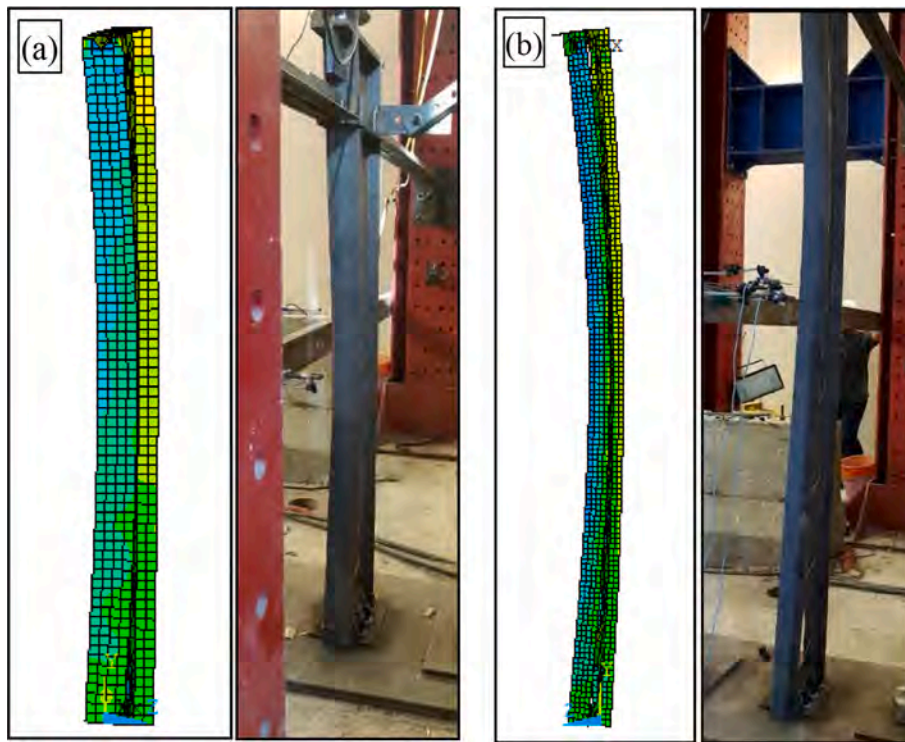


Fig. 17. Modes of failure of beam-column elements: a) short beam-columns; b) long beam-columns.

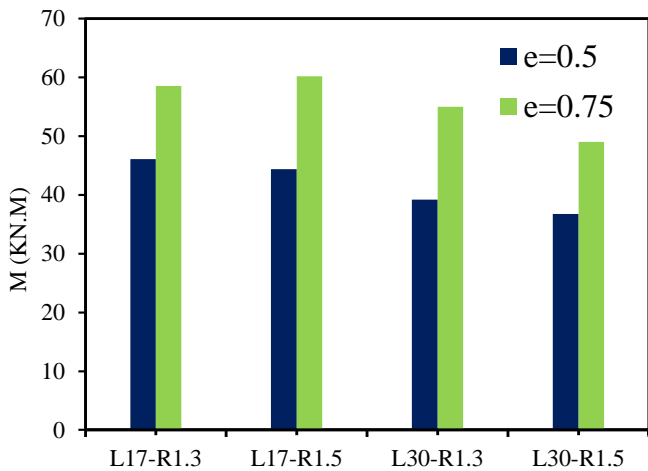


Fig. 18. Moment capacity of beam-column elements.

node element with six degrees of freedom at each node: translations in the x, y, and z axes, and rotations about the x, y, and z-axes. SHELL91 is well-suited for linear, large rotation, and/or large strain nonlinear applications. Fig. 8 shows a typical F.E mesh used for castellated element.

3.2. Boundary conditions and load application

All specimens were restrained laterally at both upper and lower end nodes. Therefore, the specimen was prevented from lateral translation at both ends. Axial load was applied to the top node of the element according to e/d ratio. To ensure the finite element model stability a mid-bottom point was restrained in x, y and z directions, top and bottom boundary conditions is shown in Fig. 9. Fig. 10 shows the finite element mesh for L17-R1.3-e0.0, L17-R1.3-e0.5 and L17-R1.3-e0.75 as examples.

3.3. Mesh convergence and initial imperfection

The finite element model results became converge when the increase in the mesh density has a neglectable effect. A total of three element sizes 10 mm, 20 mm and 30 mm are evaluated as shown in Fig. 11. The results found that the mesh size of approximately 30 mm for web and flanges provides adequate choice to be used in the modeling and save the computational time. Furthermore, initial geometric imperfections were provided in structural steel members as a result of the fabrication process. A value of $v_0 = L/500$ as suggested by Yuan et al. [19] was considered as initial imperfection in all finite element models where L is the total specimen length.

4. Finite element validation

4.1. Finite element results

Figs. 12 to 15 present comparisons between the load-displacement curves obtained from the tests and finite element analysis. Likely concluding that, the FEM can be used to predict castellated element behavior.

The ultimate axial load of each specimen obtained from both experiments and finite element modeling are presented in Table 3. It can be noticed that the ratio of experimental to the finite element capacity for all specimens' ranges between 1.0 and 1.06.

4.2. Modes of failure

Fig. 16 shows the failure mode of pure axial castellated columns obtained from both tests and finite element analysis. It can be noticed that the mode of failure of short columns is local buckling of web, where mode of failure of long columns is overall flexural buckling.

Fig. 17 shows the failure mode of eccentric beam-column elements obtained from both tests and the finite element analysis. It can be noticed that the mode of failure of short and long beam-column elements is lateral-torsional buckling.

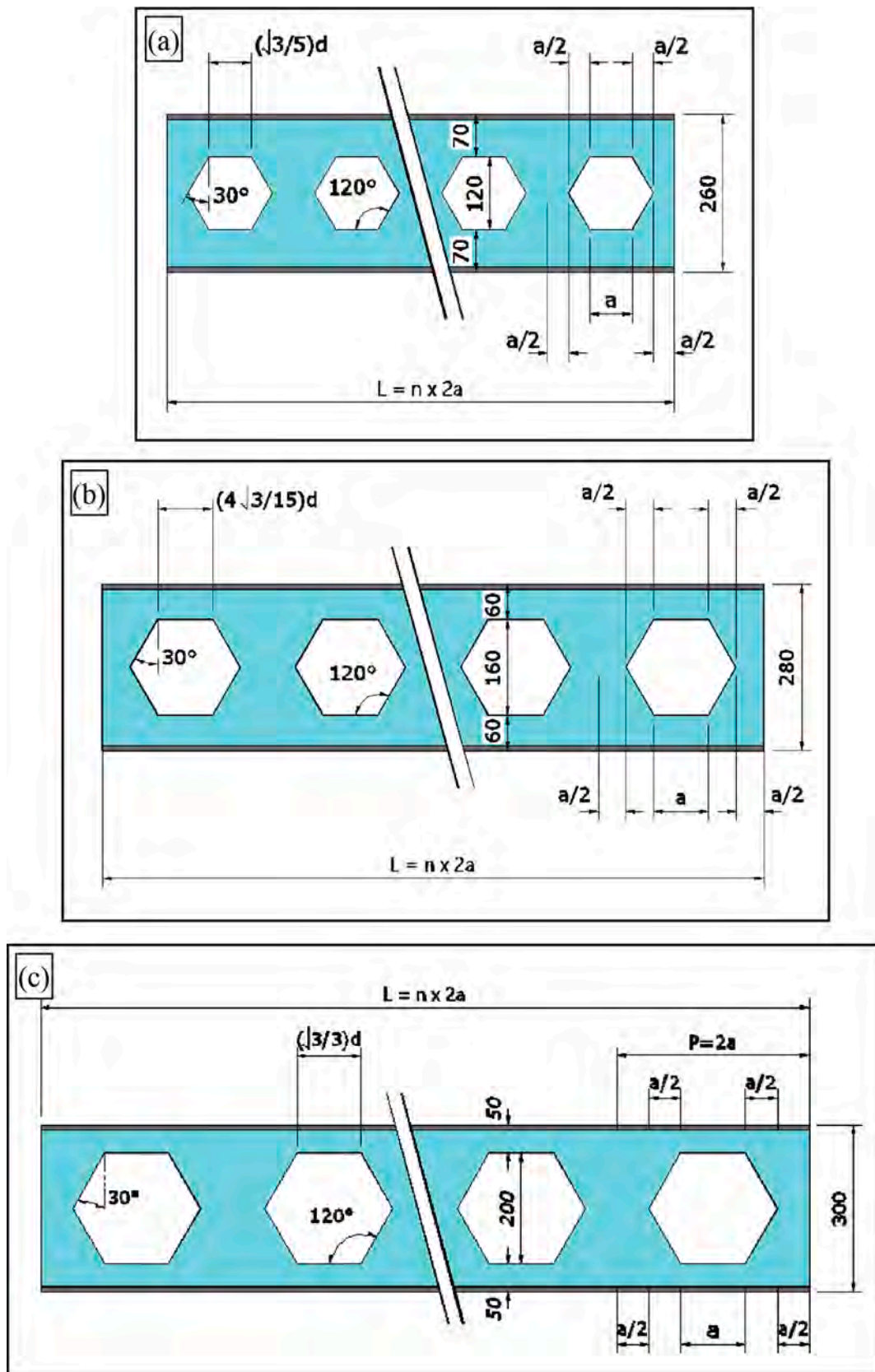
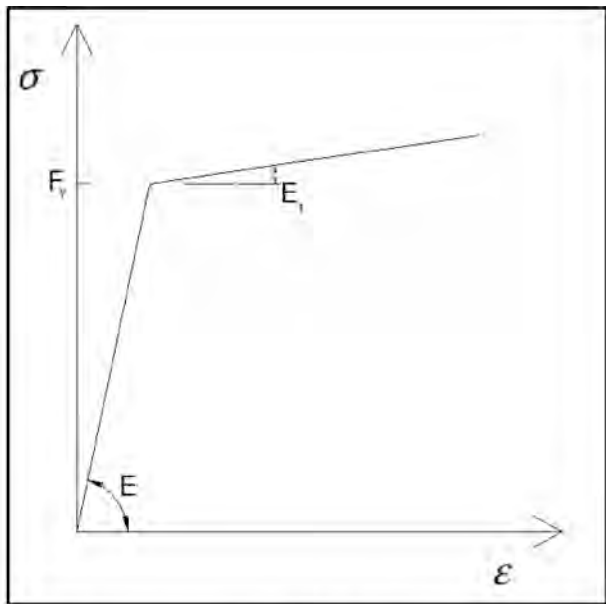


Fig. 19. Castellated element dimensions: (a) $R = 1.3$; (b) $R = 1.4$; (c) $R = 1.5$.

Table 4
Castellated elements evaluated in the parametric study.

Element Length (mm)	λ_y	Castellation Ratio [R]	(e/d)					
			0 (column)	0.25	0.5	0.75	2	infinity beam(eb)
1700	76	1(Solid Web)	L17-R1.0-e0.0	L17-R1.0-e0.25	L17-R1.0-e0.50	L17-R1.0-e0.75	L17-R1.0-e2.0	L17-R1.0-eb
			L17-R1.3-e0.0	L17-R1.3-e0.25	L17-R1.3-e0.50	L17-R1.3-e0.75	L17-R1.3-e2.0	L17-R1.3-eb
			L17-R1.4-e0.0	L17-R1.4-e0.25	L17-R1.4-e0.50	L17-R1.4-e0.75	L17-R1.4-e2.0	L17-R1.4-eb
			L17-R1.5-e0.0	L17-R1.5-e0.25	L17-R1.5-e0.50	L17-R1.5-e0.75	L17-R1.5-e2.0	L17-R1.5-eb
			L22-R1.0-e0.0	L22-R1.0-e0.25	L22-R1.0-e0.50	L22-R1.0-e0.75	L22-R1.0-e2.0	L22-R1.0-eb
2200	100	1(Solid Web)	L22-R1.3-e0.0	L22-R1.3-e0.25	L22-R1.3-e0.50	L22-R1.3-e0.75	L22-R1.3-e2.0	L22-R1.3-eb
			L22-R1.4-e0.0	L22-R1.4-e0.25	L22-R1.4-e0.50	L22-R1.4-e0.75	L22-R1.4-e2.0	L22-R1.4-eb
			L22-R1.5-e0.0	L22-R1.5-e0.25	L22-R1.5-e0.50	L22-R1.5-e0.75	L22-R1.5-e2.0	L22-R1.5-eb
			L30-R1.0-e0.0	L30-R1.0-e0.25	L30-R1.0-e0.50	L30-R1.0-e0.75	L30-R1.0-e2.0	L30-R1.0-eb
			L30-R1.3-e0.0	L30-R1.3-e0.25	L30-R1.3-e0.50	L30-R1.3-e0.75	L30-R1.3-e2.0	L30-R1.3-eb
3000	134	1(Solid Web)	L30-R1.4-e0.0	L30-R1.4-e0.25	L30-R1.4-e0.50	L30-R1.4-e0.75	L30-R1.4-e2.0	L30-R1.4-eb
			L30-R1.5-e0.0	L30-R1.5-e0.25	L30-R1.5-e0.50	L30-R1.5-e0.75	L30-R1.5-e2.0	L30-R1.5-eb
			L40-R1.0-e0.0	L40-R1.0-e0.25	L40-R1.0-e0.50	L40-R1.0-e0.75	L40-R1.0-e2.0	L40-R1.0-eb
			L40-R1.3-e0.0	L40-R1.3-e0.25	L40-R1.3-e0.50	L40-R1.3-e0.75	L40-R1.3-e2.0	L40-R1.3-eb
			L40-R1.4-e0.0	L40-R1.4-e0.25	L40-R1.4-e0.50	L40-R1.4-e0.75	L40-R1.4-e2.0	L40-R1.4-eb
4000	179	1(Solid Web)	L40-R1.5-e0.0	L40-R1.5-e0.25	L40-R1.5-e0.50	L40-R1.5-e0.75	L40-R1.5-e2.0	L40-R1.5-eb



$F_y = 240 \text{ Mpa}$ $E = 200 \text{ Gpa}$ $E_t = 1.0 \text{ Gpa}$

Fig. 20. Materials Stress-Strain Curve as suggested by Shaat [20].

4.3. Discussion of the results of the experimental work

For pure axial short columns, elements with castellation ratio ($R = 1.3$) could sustain axial load greater than those with castellation ratio ($R = 1.5$) due to the increase in section’s depth. Meaning that the effect of local buckling in the elements with castellation ratio ($R = 1.5$) is greater than elements with castellation ratio ($R = 1.3$). It can be concluded that the effect of local buckling increases by increasing the castellation ratio (R).

For pure axial long columns, elements with castellation ratio ($R = 1.3$) could sustain axial load greater than those with castellation ratio ($R = 1.5$) due to the increase in section depth, this increase in section depth increases the effect of shear deformation that occurs at the opening locations specially in the first and last openings.

Yuan et al. [19] made similar observations in their investigation, they concluded that the bearing capacity of the steel column with its expansion ratio of 1.4 is higher than the component with expansions ratio of 1.5.

For short and long beam-column elements, elements that have $e/d =$

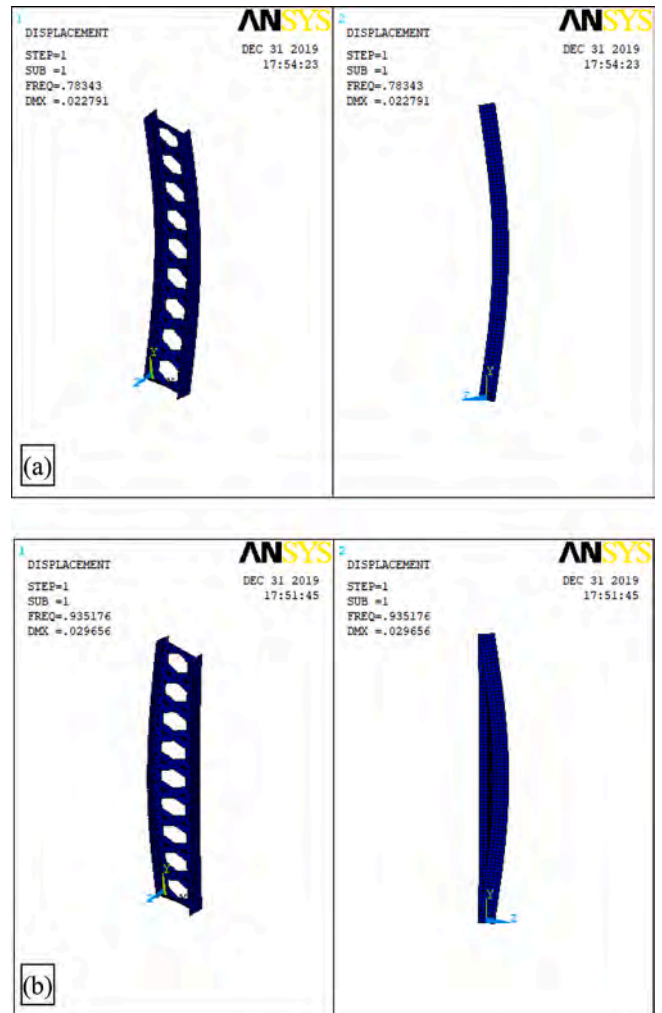
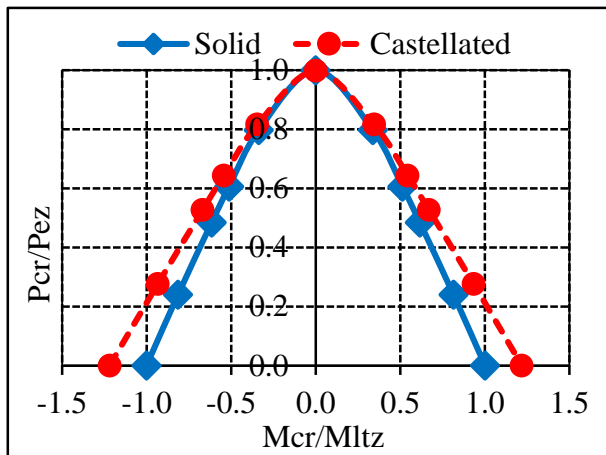
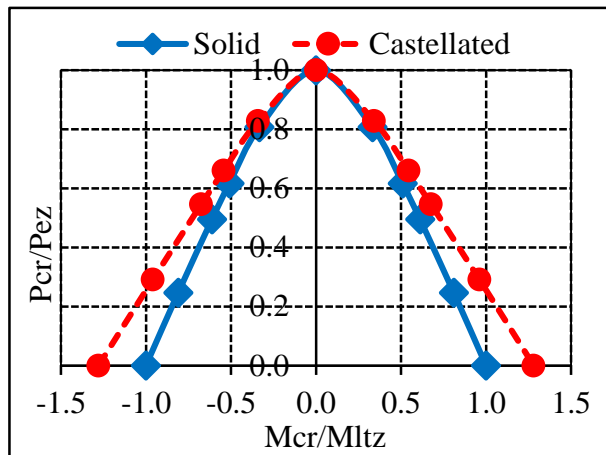


Fig. 21. Buckling mode of eccentric members: (a) concentric members; (b) eccentric members.

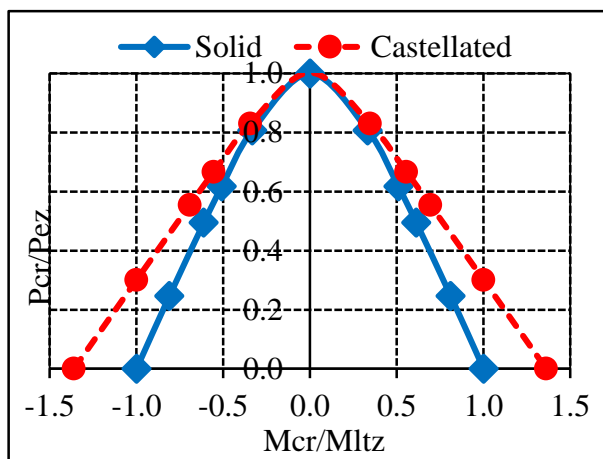
0.50 could sustain load greater than others that have $e/d = 0.75$, therefore, the increase in the eccentricity of castellated beam-column elements decreases the axial load capacity. Also, beam-column elements that have $e/d = 0.75$ could sustain bending moments greater than



a) L17&R1.3 - $P_{cr(solid)} = 928.24 \text{ KN}$ - $M_{ltz(solid)} = 109.7 \text{ KN.M}$.

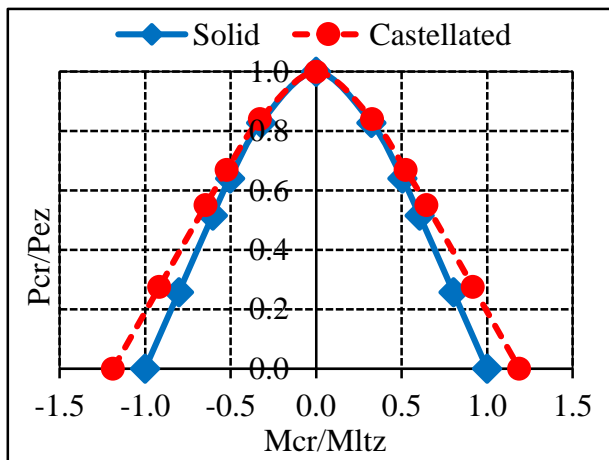


b) L17&R1.4 - $P_{cr(solid)} = 783.59 \text{ KN}$ - $M_{ltz(solid)} = 94.98 \text{ KN.M}$.

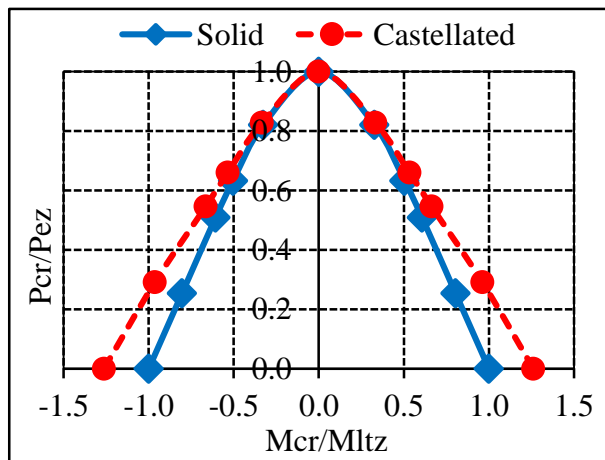


c) L17&R1.5 $P_{cr(solid)} = 827.87 \text{ KN}$ - $M_{ltz(solid)} = 99.49 \text{ KN.M}$.

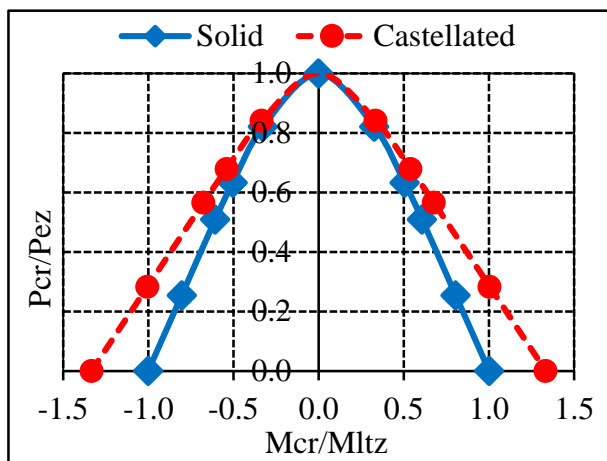
Fig. 22. Interaction diagrams for L17 elements.



a) L22&R1.3 - $P_{cr(solid)} = 579.09 \text{ KN}$ - $M_{ltz(solid)} = 74.13 \text{ KN.M}$.

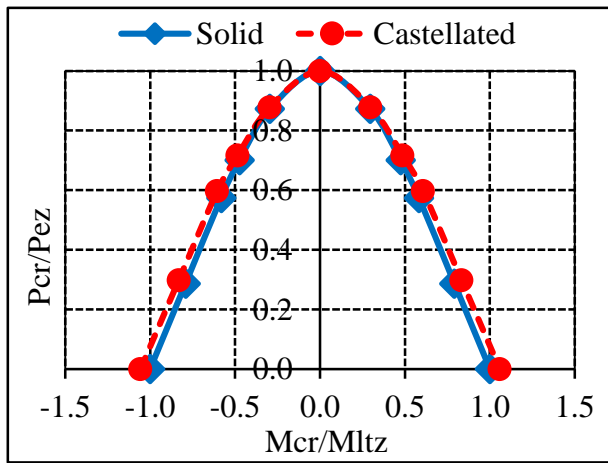


b) L22&R1.4 - $P_{cr(solid)} = 637.42 \text{ KN}$ - $M_{ltz(solid)} = 80.09 \text{ KN.M}$.

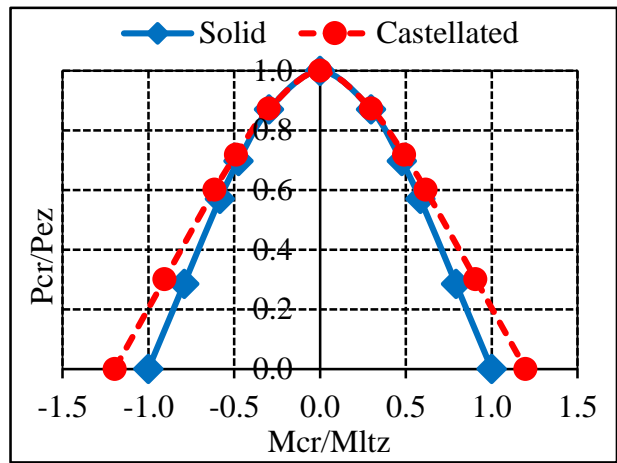


c) L22&R1.5 - $P_{cr(solid)} = 637.42 \text{ KN}$ - $M_{ltz(solid)} = 80.09 \text{ KN.M}$.

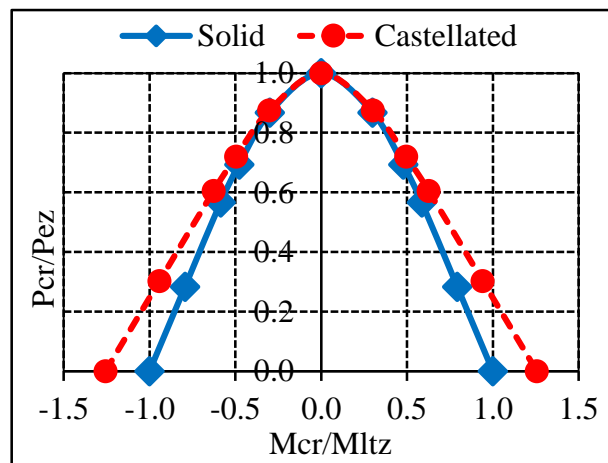
Fig. 23. Interaction diagrams for L22 elements.



a) L30&R1.3 - $P_{cr(solid)} = 316.51 \text{ KN}$ - $M_{ltz(solid)} = 46.81 \text{ KN.M}$.

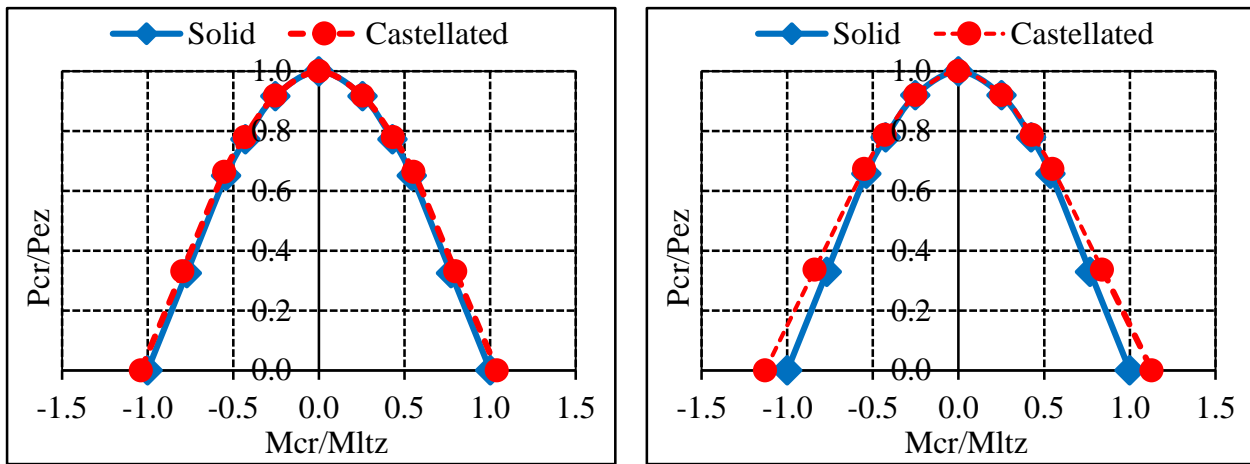


b) L30&R1.4 - $P_{cr(solid)} = 327.84 \text{ KN}$ - $M_{ltz(solid)} = 48.02 \text{ KN.M}$.

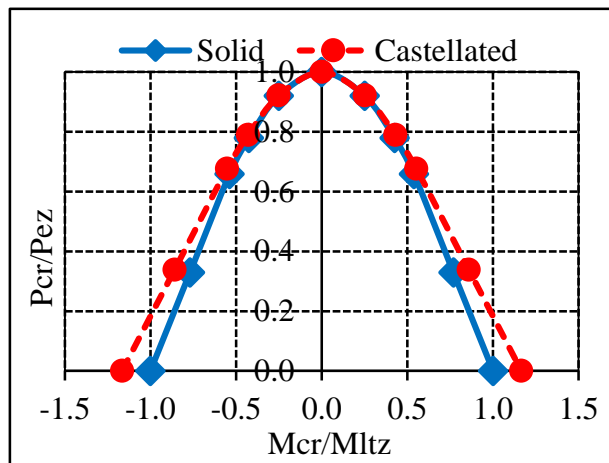


c) L30&R1.5 - $P_{cr(solid)} = 339.77 \text{ KN}$ - $M_{ltz(solid)} = 49.29 \text{ KN.M}$.

Fig. 24. Interaction diagrams for L30 elements.



a) L40&R1.3 - $P_{cr(solid)} = 169.61 \text{ KN}$ - $M_{ltz(solid)} = 30.54 \text{ KN.M}$. b) L40&R1.4 - $P_{cr(solid)} = 161.26 \text{ KN}$ - $M_{ltz(solid)} = 29.56 \text{ KN.M}$.



c) L40&R1.5 - $P_{cr(solid)} = 161.26 \text{ KN}$ - $M_{ltz(solid)} = 29.56 \text{ KN.M}$.

Fig. 25. Interaction diagrams for L40 elements.

those with $e/d = 0.5$, therefore, the increase in the eccentricity of castellated beam-column elements increases the moment capacity as shown in Fig. 18.

5. Parametric study

As indicated in section 4 of this research the results of FEA are in favorable agreement with their experimental counterpart. Therefore, it was decided to use the finite element analysis as a tool to perform the current parametric study.

5.1. Geometric properties

An IPE200 cross section was used in the study with the standard section dimensions (flange pls 100*8.5 mm and web 5.6 mm thickness in total depth of 200 mm). Three castellation ratios (R) were investigated in the study 1.3, 1.4 & 1.5 Fig. 19 illustrates the different section dimensions used in the study.

Table 4 illustrates element length, out of plan slenderness ratio, castellation ratio (R) and (e/d) ratio for different elements investigated in the study.

5.2. Material definitions

The first stage of the numerical solution was essentially a linear elastic analysis of the control element, in which the structure stiffness remained unchanged. Accordingly, the value of Young's modulus ($2e + 8 \text{ KN/m}^2$) and passion's ratio of steel (0.3) was defined. On the other hand, the second stage of the numerical simulation comprised a non-linear analysis, where the stiffness of the structure has change during deformation. The steel non-linearity (plasticity) was accounted in the FEM by specifying a bi-linear isotropic hardening model. As shown in Fig. 20, the tangent modulus of steel was assumed equal to 0.5 percent of its elastic modulus as suggested by Shaat [20].

5.3. Finite element analysis result

5.3.1. Linear buckling analysis result

Weak-axis flexural buckling was the governing buckling mode for all pure axial elements, whereas lateral-torsional buckling was the governing buckling mode for beams. For beam-columns, the buckling modes seemed as a combination of flexural buckling and lateral-torsional buckling. Fig. 21 shows the buckling mode for concentric and eccentric castellated elements.

Figs. 22 to 25 show a comparison between the interaction linear

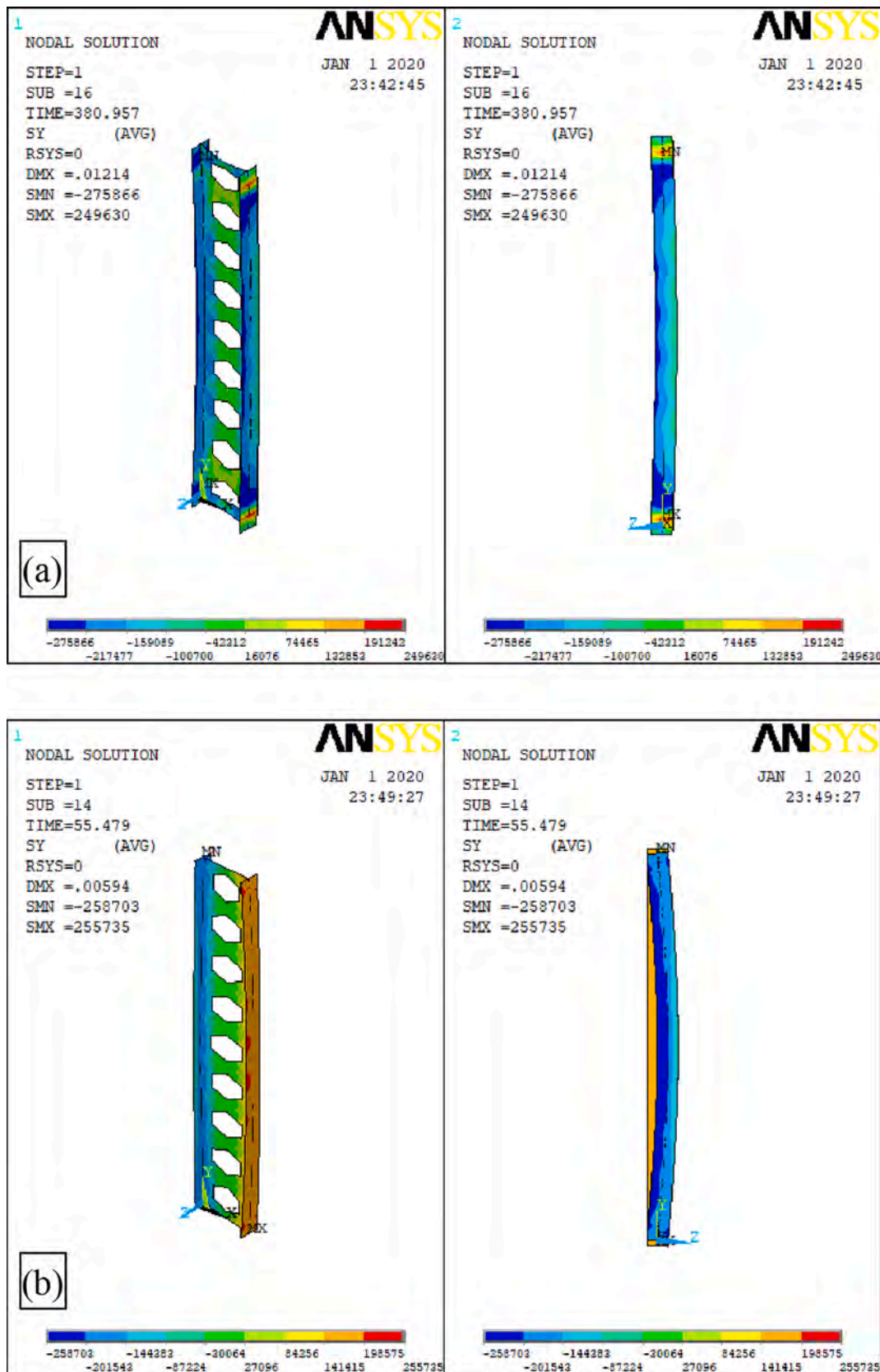


Fig. 26. Stresses for concentric-eccentric elements: (a) concentric member's stresses; (b) eccentric member's stresses.

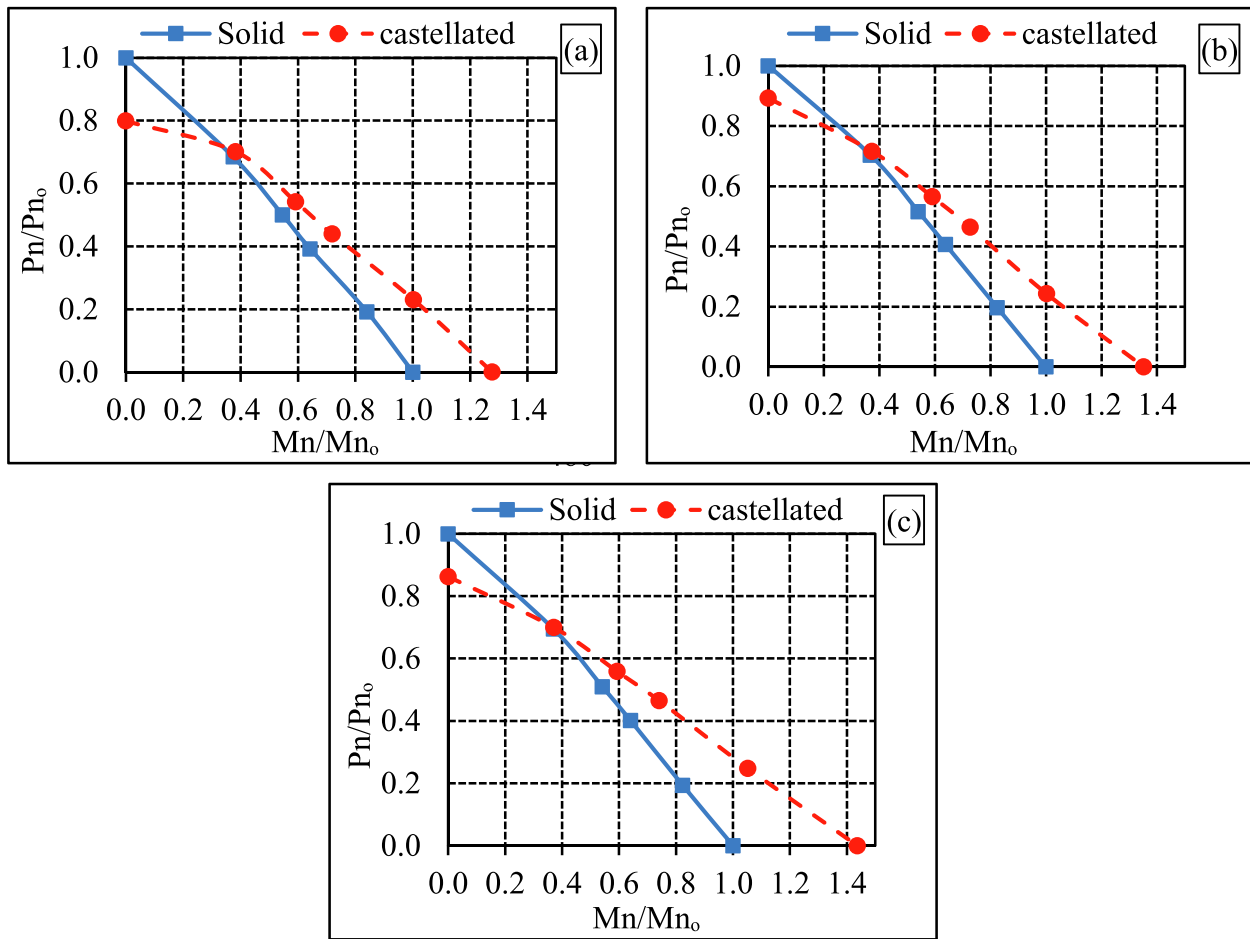


Fig. 27. Interaction diagrams for L17 elements: (a) R = 1.3; (b) R = 1.4; (c) R = 1.5.

buckling diagrams of solid and castellated elements for the studied spans and castellations ratios (R). Horizontal axes present the ratio between M_{cr}/M_{ltz} where, M_{cr} is the critical bending load of either castellated or solid web element and M_{ltz} is the critical bending load of the solid web element. The vertical axes present the ratio between P_{cr}/P_{ez} where, P_{cr} is the critical buckling load of either castellated or solid web element and P_{ez} is the critical buckling load of the solid web element.

5.3.1.1. Impact of (e/d) ratio. Figs. 22 to 25 indicate that increasing the (e/d) ratio contributes to increased M_{cr}/M_{ltz} and decreased P_{cr}/P_{ez} , regardless of the castellations ratio (R). For elements under pure axial force (L17 elements), increasing the castellations ratio (R) from 1.3 to 1.4 and 1.5, changes the value of P_{cr}/P_{ez} from 0.998 to 1.0 and 1.003 respectively. Accordingly, the castellations ratio (R) indicates a negligible effect on the critical buckling load for the elements under pure axial force due to the shear deformation that may occur at opening locations. Yuan et al. [6] made similar observations in their investigation of the shear deformations that occur at the opening location, they concluded that the inclusion of web shear deformation reduces the buckling resistance of castellated columns. Therefore, the existence of the openings along the web of the castellated column elements results in decreasing the column capacity.

Also, Gu and Cheng [8] concluded that web shear deformation in cellular columns can significantly reduce the buckling resistance of the column and ignoring the shear deformation effect will normally over predict the ability of the column against buckling about its major axis.

However, for elements under pure bending, increasing the castellations ratio (R) from 1.3 to 1.4 and 1.5 results in an increase from 1.218 to 1.28 and 1.316, respectively. Therefore, the castellations ratio (R)

indicates a considerable effect on the critical buckling load for the elements under pure bending. Elaiwi et al. [14] made similar observation in their study, they concluded that the critical load of lateral-torsional buckling of castellated beams is influenced by web openings.

While, for the beam-column elements with a castellations ratio (R) of 1.3, the P_{cr}/P_{ez} has been decreased from 0.816 to 0.276 and M_{cr}/M_{ltz} increased from 0.345 to 0.934 by increasing the (e/d) ratio from 0.25 to 2.0. For the beam-column elements with a castellations ratio (R) of 1.4, the P_{cr}/P_{ez} has been decreased from 0.828 to 0.291 and M_{cr}/M_{ltz} increased from 0.341 to 0.961 by increasing the (e/d) ratio from 0.25 to 2.0. Finally, for the beam-column elements with a castellations ratio (R) of 1.5, the P_{cr}/P_{ez} has been decreased from 0.830 to 0.301 and M_{cr}/M_{ltz} increased from 0.045 to 1.000 by increasing the (e/d) ratio from 0.25 to 2.0.

As can be seen in Figs. 22–25, that increasing the castellations ratio (R) increases the critical buckling moment. On the other hand, the castellated elements experienced P_{cr}/P_{ez} ratio close to unity, therefore, the castellations ratio (R) shows a negligible effect on the critical buckling load.

Additionally, increasing the (e/d) ratio increases the critical buckling moment and decreases the critical buckling load. On the other hand, element length has a considerable effect on the critical buckling moment, increasing the element length decreases the critical buckling moment due to the effects of the lateral-torsional buckling.

5.3.2. Nonlinear buckling analysis result

Nonlinear buckling analysis was performed to predict the failure load for each castellated element. Weak-axis flexural buckling was the governing mode of failure for all pure axial elements, whereas lateral-

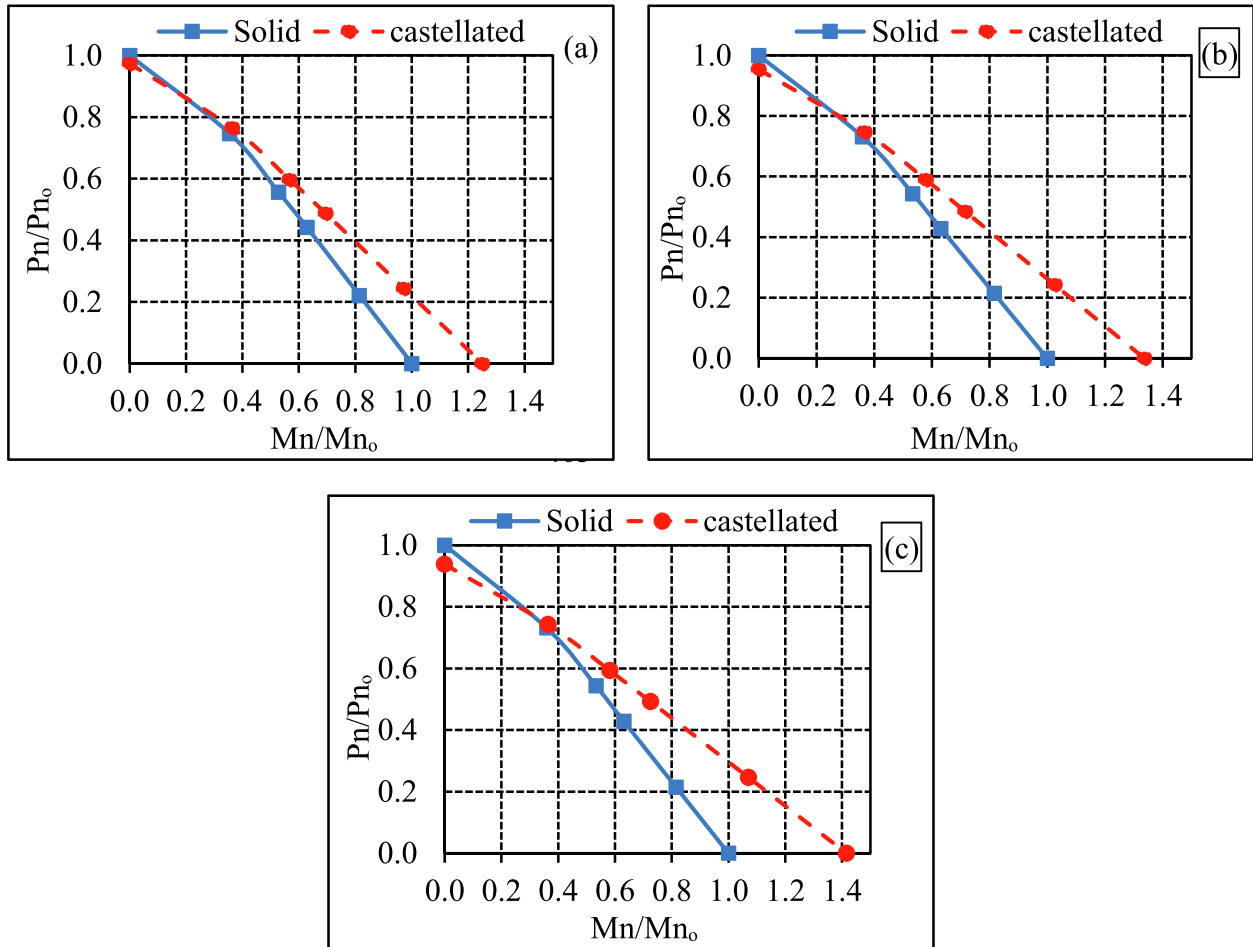


Fig. 28. Interaction diagrams for L22 elements: (a) $R = 1.3$; (b) $R = 1.4$; (c) $R = 1.5$.

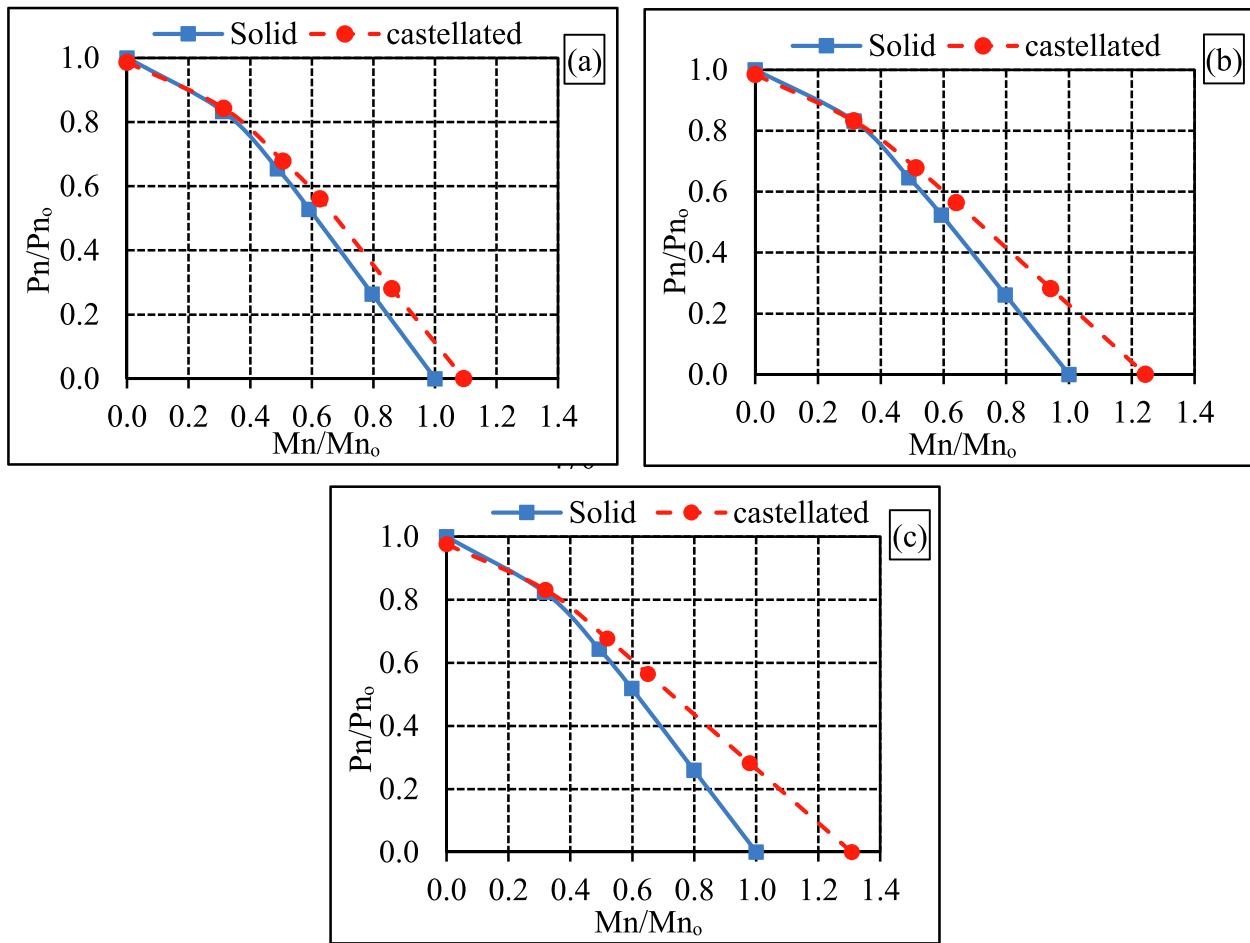


Fig. 29. Interaction diagrams for L30 elements: (a) R = 1.3; (b) R = 1.4; (c) R = 1.5.

torsional buckling was the governing mode of failure for beams. For beam-columns, the mode of failure seemed as a combination of flexural buckling and lateral-torsional buckling. Fig. 26 shows the buckling mode for concentric and eccentric castellated elements.

Figs. 27 to 30 show a comparison between the interaction diagrams of solid and castellated elements for the studied spans and castellations ratios (R). Horizontal axes present the ratio between M_n/M_{n0} where, M_n is either castellated or solid web element bending strength and M_{n0} is the solid web element bending strength. The vertical axes present the ratio between P_n/P_{n0} where, P_n is either castellated or solid web element axial strength and P_{n0} is the solid web element axial strength.

5.3.2.1. Impact of (e/d) ratio. Figs. 27 to 30 indicate that, increasing the (e/d) ratio increases M_n/M_{n0} and decreases P_n/P_{n0} , regardless of the castellations ratio (R). For elements under pure axial force (L17 elements), increasing the castellations ratio (R) from 1.3 to 1.4 and 1.5, changes the value of P_n/P_{n0} from 0.799 to 0.893 and 0.863, respectively. Accordingly, castellations decreases the axial capacity compared to the solid web elements.

For short elements (L17 and L22), castellations decreases the axial capacity for different castellations ratio (R) due to the effect of shear deformation that occurs at the opening locations along the castellated column web especially at the first and last openings as shown in Fig. 31.

Otherwise, for long elements (L = 30 and L40), the capacity of the elements in axial are close to the solid web element and the mode of failure is the flexural buckling mode of failure as shown in Fig. 32.

However, for elements under pure bending, increasing the castellations ratio (R) from 1.3 to 1.4 and 1.5 results in an increase in M_n/M_{n0} from 1.277 to 1.353 and 1.437, respectively. Therefore, the castellations

ratio (R) shows/showed a considerable effect on the bending capacity for elements under pure bending. Also, the increase in castellations ratio (R) increases the bending capacity. This explains the fact that, increasing the section depth leads to an increase in the moment of inertia I_x and the section modulus S_x without any increase in the element weight.

While, for the beam-column elements with a castellations ratio (R) of 1.3, the P_n/P_{n0} has been decreased from 0.701 to 0.230 and M_n/M_{n0} increased from 0.383 to 1.003 by increasing the (e/d) ratio from 0.25 to 2.0. For the beam-column elements with a castellations ratio (R) of 1.4, the P_n/P_{n0} has been decreased from 0.715 to 0.243 and M_n/M_{n0} increased from 0.375 to 1.003 by increasing the (e/d) ratio from 0.25 to 2.0. Finally, for the beam-column elements with a castellations ratio (R) of 1.5, the P_n/P_{n0} has been decreased from 0.699 to 0.248 and M_n/M_{n0} increased from 0.372 to 1.053 by increasing the (e/d) ratio from 0.25 to 2.0.

5.3.2.2. Castellations enhancement (η). Enhancement diagrams were plotted for each element length to investigate the best castellations ratio as shown in Fig. 33. The diagrams were plotted between enhancement (η) on the vertical axis and the (e/d) ratio on the horizontal axis. Six (e/d) ratios were considered, 0, 0.25, 0.5, 0.75, 2.0 and ∞ . Moreover, three castellations ratios (R) were considered, 1.3, 1.4 and 1.5.

Enhancement (η) is the ratio between the following:

$$\sqrt{\left(\frac{M_n}{M_{n0(solid)}}\right)^2 + \left(\frac{P_n}{P_{n0(solid)}}\right)^2}, \text{ for castellated elements, and}$$

$$\sqrt{\left(\frac{M_{n(solid)}}{M_{n0(solid)}}\right)^2 + \left(\frac{P_{n(solid)}}{P_{n0(solid)}}\right)^2}, \text{ for solid web elements, where:}$$

M_n equals to castellated element bending capacity, P_n equals to

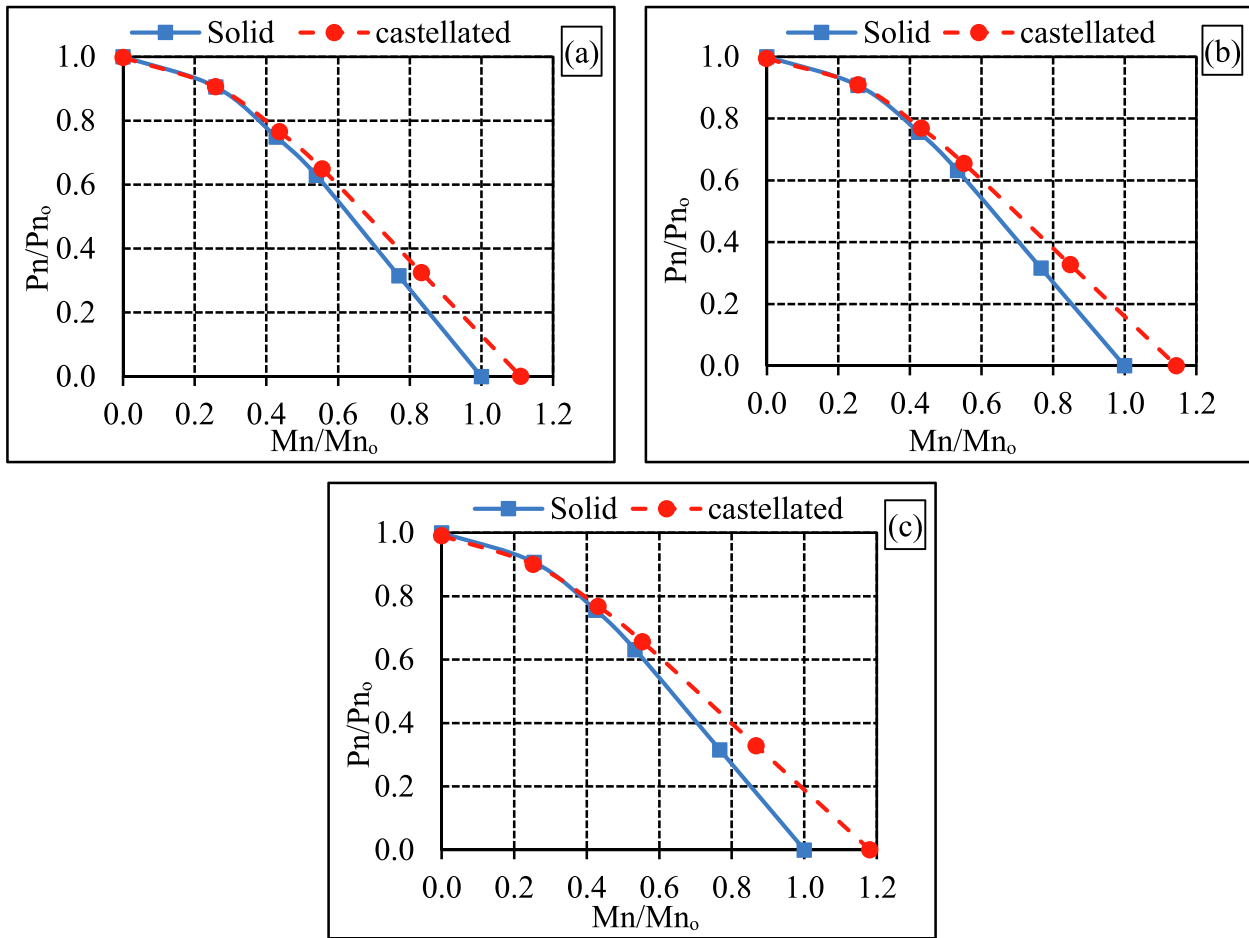


Fig. 30. Interaction diagrams for L40 elements: (a) $R = 1.3$; (b) $R = 1.4$; (c) $R = 1.5$.

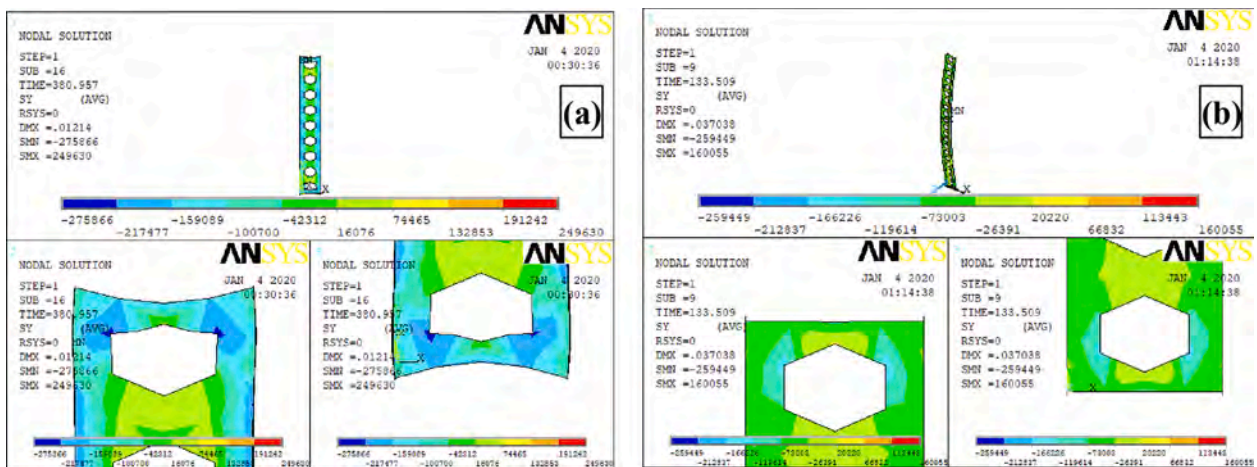


Fig. 31. Effect of first&last opening for short&long elements: (a) short elements; (b) long elements.

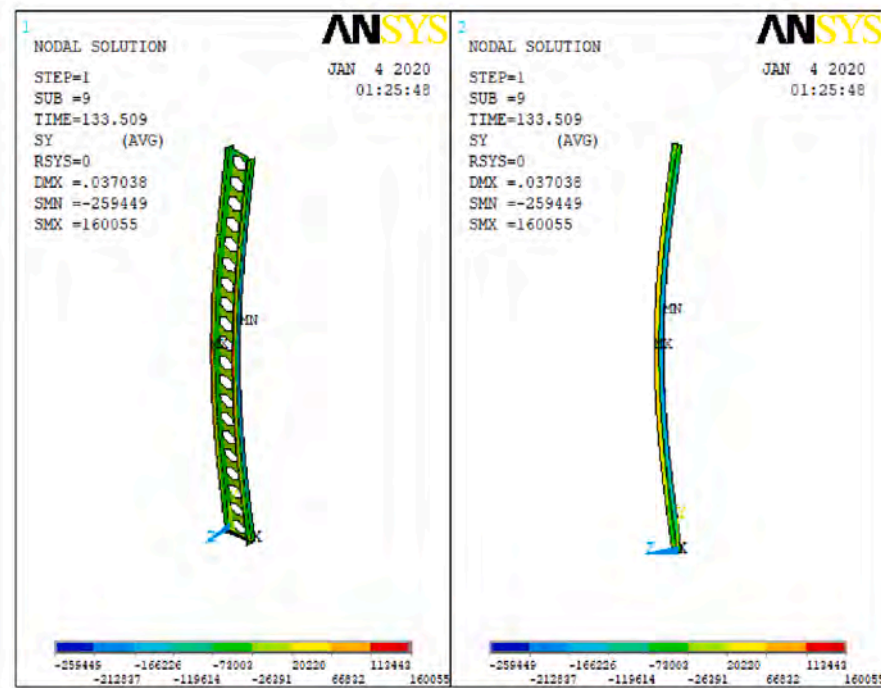


Fig. 32. Lateral-torsional buckling of short&long elements.

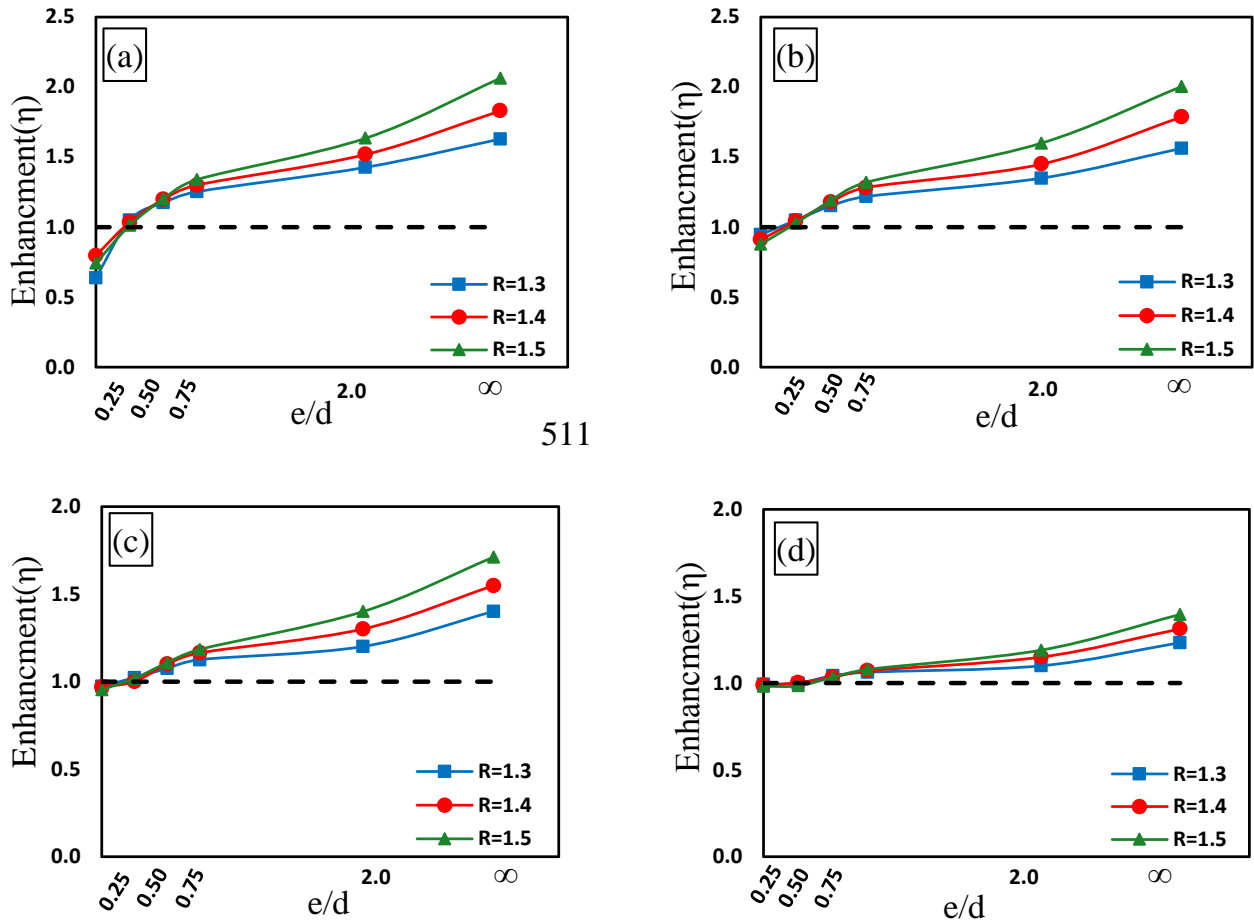


Fig. 33. Variation of strength enhancement ratio (η) with the eccentricity ratio (e/d): (a) L17; (b) L22; (c) L30; (d) L40.

castellated element axial capacity and $M_{no(solid)}$ equals to solid web element pure bending capacity, $P_{no(solid)}$ equals to solid web element pure axial capacity.

And, $M_{n(solid)}$ equals solid web element bending capacity and $P_{n(solid)}$ equals to solid web element axial capacity.

Fig. 33 shows that for L17 and L22 elements when $(e/d) = 0.0$, the enhancement curve is below the unity curve, therefore, for these elements' castellated decreases the element capacity, also, for $(e/d) = 0.25$, the enhancement curve is close to the unity curve, therefore, for these elements' castellated does not increase the element capacity. Whereas from $(e/d) = 0.5$ to ∞ , the enhancement curve is above the unity curve, therefore, for these elements, castellated increases the element capacity.

Also, for L30 and L40 elements, when $(e/d) = 0.0$ and 0.25 , the enhancement curve is close to the unity curve, therefore, for these elements' castellated does not increase the element capacity, whereas, from $(e/d) = 0.5$ to ∞ , the enhancement curve is above the unity curve, therefore, for these elements, castellated increases the element capacity.

For (L17 elements), increasing the castellated ratio (R) from 1.3 to 1.4 and 1.5, changes the value of enhancement (η) from 1.63 to 1.83 and 2.06, respectively. Accordingly, the elements that have castellated ratio (R) = 1.5 have the best enhancement (η) value. Also, increasing elements length decreases the enhancement (η) due to the effects of the lateral-torsional buckling.

6. Conclusions

This paper reports on experimental and finite-element investigation of the structural behavior of castellated elements; including columns, beams, and beam-columns. Based on the experimental results and the parametric study using the finite-element verified model presented in this paper, the following conclusions can be drawn:

The developed finite-element model using ANSYS has provided accurate simulations of the experimental response of the tested castellated elements. The castellated has no effect on the linear buckling load for elements subjected to pure axial loading. Otherwise, the castellated ratio has significantly affected the linear buckling moment of the pure bending elements.

For beam-column elements, increasing the (e/d) ratio has increased the linear buckling moment from 0.341 to 1.00 and decreased the linear buckling load from 0.816 to 0.276. Also, element length has a considerable effect on both the linear buckling load and moment, the increase in the element length decreases the linear buckling load and moment due to the effects of lateral-torsional buckling.

By performing a non-linear analysis on pure axial elements, the value of P_n/P_{no} ranged from 0.799 to 0.893 for the different castellated ratios. As a result, the capacity of the castellated elements has been decreased when compared to solid web elements due to the effect of shear deformation, especially at the first and last openings. The governing mode of failure of long elements was flexural buckling mode for both the castellated and solid web elements.

For pure bending elements, increasing the castellated ratio has resulted in an increase in M_n/M_{no} ranged from 1.277 to 1.437. Therefore, the castellated ratio (R) shows a considerable effect on the bending capacity for the elements under pure bending. For the beam-column elements (L17 elements), the ratio of P_n/P_{no} has been decreased from

0.699 to 0.230 and M_n/M_{no} increased from 0.372 to 1.053 by an increase in the (e/d) ratio. Therefore, increasing (e/d) ratio has increased the moment capacity and decrease the axial capacity of castellated beam-column elements.

The castellated process increases the major axis inertia of the section, but does not affect the minor axis inertia. Pure bending strength is mainly governed by the major axis inertia, particularly for beams restrained against lateral-torsional buckling. On the other hand, pure axial capacity is governed by the section area and minor axis inertia. Accordingly, castellated process significantly enhances pure bending strength, but does not enhance the pure axial strength. However, for beam-columns, the strength enhancement ratio depends on the eccentricity ratios (e/d) . As can be concluded from Fig. 33, beam-columns strength does not improve for $e/d < 0.25$. For $e/d > 0.25$, the strength starts to improve until it reaches its maximum enhancement ratio at $e/d = \infty$, i.e., for pure bending.

Declaration of Competing Interest

The authors declare that they have no known competing financial interests or personal relationships that could have appeared to influence the work reported in this paper.

References

- [1] Mohebkah A, Showkati H. Bracing requirements for inelastic castellated beams. *J Constr Steel Res* 2005;61:1373–86.
- [2] Showkati H. Lateral-torsional buckling of castellated beams. *Iran J Sci Technol, Trans B, Eng* 2008;2(B2):153–6.
- [3] Ellobody E. Interaction of buckling modes in castellated steel beams. *J Constr Steel Res* 2011;67:814–25.
- [4] Ellobody E. Nonlinear analysis of cellular steel beams under combined buckling modes. *Thin-Walled Struct* 2012;52:66–79.
- [5] Abu-Sena ABB, Soliman MS, Abdel-Nabi ONA. Behavior and resistance of beam-column structural elements. *J Constr Steel Res* 2012;71:171–81.
- [6] Yuan W, Kim B, Li L. Buckling of axially loaded castellated steel columns. *J Constr Steel Res* 2014;92:40–5.
- [7] Kumbhar PD, Jamdar AM. Optimization of opening size for castellated beam with sinusoidal openings. *Int J Optimiz Civil Eng* 2015;5(3):301–13.
- [8] Gu J, Cheng S. Shear effect on buckling of cellular columns subjected to axially compressed load. *Thin-Walled Structures* 2016;98:416–20.
- [9] Shaikh A, Autade P. Structural analysis and design of castellated beam in cantilever action. *Int Res J Eng Technol* 2016;3(8):163–70.
- [10] Sonck D, Belis J. Weak-axis flexural buckling of cellular and castellated columns. *J Constr Steel Res* 2016;124:91–100.
- [11] Wang P, Guo K, Liu M, Zhang L. Shear buckling strengths of web-posts in a castellated steel beam with hexagonal web openings. *J Constr Steel Res* 2016;121:173–84.
- [12] Yuan W, Yu N, Bao Z, Wu L. Deflection of castellated beams subjected to uniformly distributed transverse loading. *Int J Steel Struct* 2016;16(3):813–21.
- [13] Elaiwi S, Kim B, Li L. Bending analysis of castellated beams, *Athens J Technol Eng*, 6 (1) (2019).
- [14] Elaiwi S, Kim B, Li L. Linear and nonlinear buckling analysis of castellated beams, *Int J Struct Civil Eng Res*, 8 (2) (2019), 83–93.
- [15] Hadeed SM, Alshimmeri AJH. Comparative study of structural behavior for rolled and castellated steel beams with different strengthening techniques. *Civil Eng J* 2019;5(6):1384–94.
- [16] Serene KT, Aswathy P. Finite element analysis of composite beams and columns with castellated members. *Int J Sci Eng Res* 2019;10(5):429–35.
- [17] Liu M, Liang M, Ma Q, Wang P, Ma C. Web-post-buckling of bolted castellated steel beam with octagonal web openings. *J Constr Steel Res* 2020;164:1–15.
- [18] ANSYS verification manual. Release 12.0. United States Inc; 2009.
- [19] Yuan X, Liu F, Li Z, Xu Y. Finite element analysis for castellated steel columns with two different expansion ratios. *IEEE* 2012:2589–92.
- [20] Shaat AA. Structural behavior of steel columns and steel-concrete composite girders retrofitted using CFRP, [Doctor of philosophy thesis]. Queen's university Kingston, Ontario, Canada, November (2007).